1991

Determination of the thermal properties of thin polymer films

Duane A. Swanson

DETERMINATION OF THE THERMAL PROPERTIES OF THIN POLYMER FILMS

by
Duane A. Swanson

A Thesis Submitted
in
Partial Fulfillment
of the
Requirements for the Degree of
MASTER OF SCIENCE
in Mechanical Engineering
at
Rochester Institute of Technology

Approved by:

Dr. Joseph S. Torok, Thesis Co-Advisor
Mechanical Engineering Department
Rochester Institute of Technology

Dr. Ali Ogut, Thesis Co-Advisor
Mechanical Engineering Department
Rochester Institute of Technology

Dr. Alan Nye
Mechanical Engineering Department
Rochester Institute of Technology

Mr. Richard Cianciotto
Manager of Process Technology Department
Mobil Chemical Company, Films Division

Dr. Charles Haines, Department Head
Mechanical Engineering Department
Rochester Institute of Technology

I, Duane A. Swanson, do hereby grant permission to Wallace Memorial Library, of R.I.T., to reproduce my thesis in whole or part. Any reproduction will not be used for commercial use or profit.

ACKNOWLEDGEMENT

To Mobil Chemical Company, Films Division, especially Richard Cianciotto and Sharon Kemp-Patchett, for their support and initiating this research work with R.I.T., I express sincere gratitude.

To R.I.T. Mechanical Engineering Faculty Members, who have instilled me with vast knowledge and experience throughout my college career, many thanks.

To Dr. Joseph S. Torok, my professor, advisor, mentor, and friend, I express deepest gratitude and appreciation.

To my Mother and Father, my appreciation for providing support and encouragement to allow me to achieve.

Most of all, I would like to thank my wife, Nancy. For her patience, understanding, and love, I dedicate this work.

ABSTRACT

The purpose of this investigation was to analyze heat transfer characteristics of cavitated-core polymer films. The effects of thickness and composition on the insulative properties of thin polymer films were studied.

Two experimental tests were developed to measure the heat transfer rate through a variety of thin films. One test apparatus was used to study convective and radiative effects while the second was used to study the conductive effects.

A finite element model of a frozen food commodity wrapped in an insulative thin film was developed. Transient simulations were performed for the dynamic characterization of thermal wave propagation across the film layer. This model was then used to compare insulative properties associated with various packaging films.

Experiments established that radiation effects are very significant in the freezer environment. Experiments also verified that cavitated-core films were more insulative than solid films. Modeling results illustrated that thickness and conductivity of a thin film only have insulative significance when exposed to a purely conductive environment.

TABLE OF CONTENTS

TABLES

FIGURES

FIGURES

Nomenclature

A_s surface area, m^2
C_p specific heat, J/kgK
D depth, m
$\dot{E}_g$ rate of energy generation, W
$\dot{E}_{in}$ rate of energy transfer into a control volume, W
$\dot{E}_{out}$ rate of energy transfer out of a control volume, W
$\dot{E}_{st}$ rate of increase in internal stored energy, W
h convection heat transfer coefficient, W/m^2K
$\bar{h}$ average convection heat transfer coef.,W/m^2K
k thermal conductivity, W/mK
L length, m
q heat transfer rate, W
q" heat flux, W/m^2
T temperature, K
t time, s
V Volume, m^3

Greek Letters
α thermal diffusivity, m^2/s
Γ boundary conditions
ϵ emissitivity, m^2/s
σ Stefan-Boltzman constant (5.67E-08 W/m^2K^4)
ρ mass density, kg/m^3
Φ appropriate functions
Ω domain

```
" DETERMINATION OF THE THERMAL PROPERTIES OF POLYMER THIN FILMS    "
"                                                                  "
" Program : Freeze10 : ACSL : RIT VAX/VMS                         "
" Programmer : Duane A. Swanson                                   "
"                                                                  "
" Abstract : The ACSL program solves a system of ten differential "
" equations that represent a Finite Element Model designed to     "
" estimate the transient heat transfer of a frozen commodity      "
" wrapped in an insulating film and subjected to various inputs.  "


PROGRAM FREEZE10

DERIVATIVE

      "-----------------------DEFINE PRESET VARIABLES"

      CONSTANT        TSTP = 1200., ...
                      T2O = -1.,...
                      T6O = -1.,  T10O= -1.,...
                      T3O = -1.,   T7O = -1.,  T11O= -1.01,...
                      T4O = -1.,   T8O = -1.,...
                      T5O = -1.,   T9O = -1.,...
                      HE = .015,...
                      DELTAX = 2.45E-05,...
                      PI = 3.14159,...
                      ALPHA = 3.09E-07,...
                      KF = .10,...
                      TAVE = -1.,...
                      TAMP = 5.,...
                      KAIR = 24.3E-03,...
                      HAIR = 2.5,...
                      E = .1,...
                      A = .2,...
                      RHOC = 3.33E6

      CINTERVAL       CINT = 1.

      "-----------------------"

      C1 = ALPHA/(HE)
      C2 = 6./(HE*100.)
      MT = T/60


" Vario environmental inputs the model can be subjected to.       "

      "CASE 1 HARMONIC INPUT"
      "TINF = TAVE  + TAMP*SIN(T*3.14159/600)"

      "CASE 2 TINF  STEP INPUT "
      "Y = PULSE(0.,1200.,200.)  "
      "X = PULSE(200.,2400.,800.) "
      "Z = PULSE(1000.,3600.,400.) "
      "TINF = TAVE + (1.5)*Y*MT + X*TAMP - (.75)*Z*(MT-10.) "
```

1.0 INTRODUCTION

Polymer plastic films are widely used in packaging of food commodities. These films are becoming ever more popular, due to ease of manufacturing and printability, for prolonging product shelf-life. Many of the films used in the packaging of freezer and refrigerator commodities consist of a solid polymer. A new packaging substrate has been developed consisting of several layers in which a cavitated core is sandwiched between two solid film layers. This composite structure manufactured by a cavitating process is hypothesized to provide better thermal protection.

This approach is different compared to past packaging film development in that thermal protection is included in the design of the composite layers. Most of the previous design considerations have focused on tensile and puncture strength, printability, and water vapor transmission properties.

The objective of this work was to carry out an experimental and theoretical study to investigate the thermal characteristics of composite films such as cavitated OPPalyte(™), white polyethylene, clear coextruded polypropylene, and metallized films in comparison to other conventional packaging materials. The thermal response to all three modes of heat transfer, i.e. convection, conduction, and radiation, will be considered.

Using the Finite Element Method, the mechanism of heat transfer through a film is mathematically modeled. With this model,

the experimental setup will be verified by establishing a high level of confidence. Further, apparent conductivities will be found for typical composite films. Once these thermal parameters are set, one can use a model that simulates a frozen commodity wrapped in an insulative film subject to various freezer environments (i.e. freezer cycling or temperature shock). This modelling allows for comparison of different films (solid, cavitated, metallized, etc..) with respect to their insulative properties and effectiveness in storing frozen commodities.

2.0 Theory and Literature Review:

2.1 Heat Transfer Theory :

Heat is transported through a medium (gas, liquid, or solid) due to a temperature difference at two different points. Heat flows from a high temperature region to a low temperature region. Temperature is fundamentally a potential field denoting the relative energy of the substance [1]. This transmission of energy takes place in three modes : conduction, convection and radiation as depicted below (See Figure 2.1).

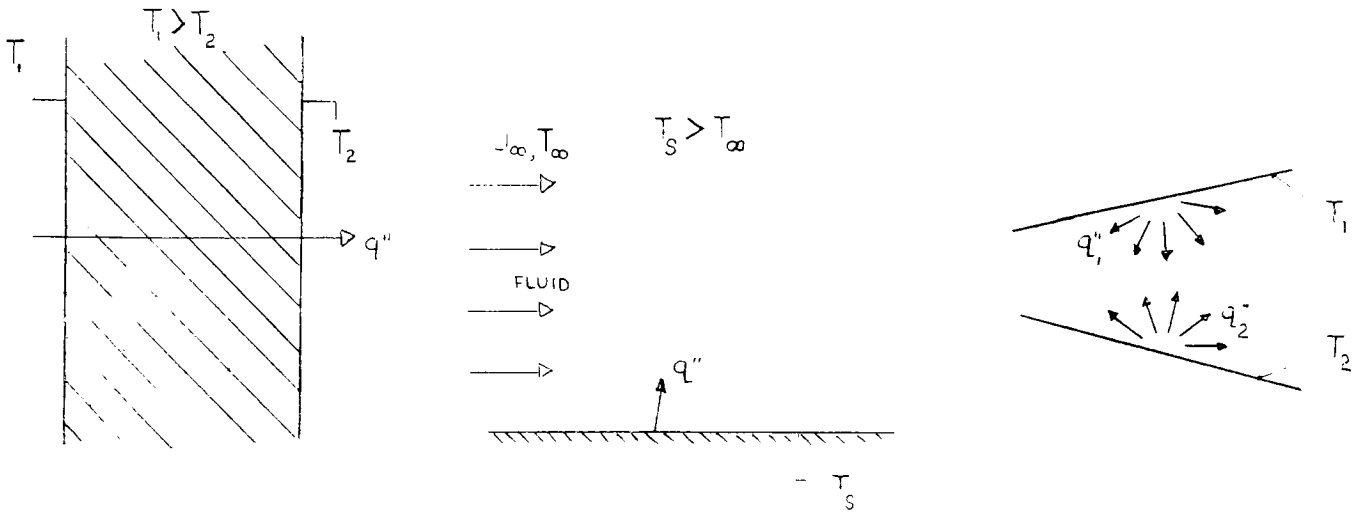

Conduction Convection Radiation

Figure 2.1
Modes of Heat Transfer

Conduction

Heat Conduction denotes the transport of energy as a result of molecular interactions under the influence of a nonhomogeneous temperature distribution.

Consider a homogeneous medium in which a temperature distribution exists, $T(x,y,z)$. By applying the conservation of energy to an infinitesimally small control volume, $dx*dy*dz$, the governing equation of heat conduction may be derived.

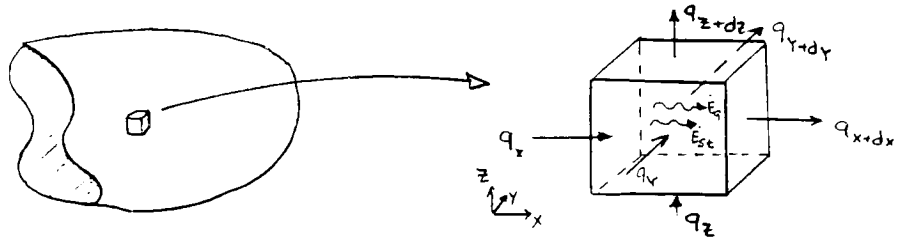

Figure 2.2
Differential Control Volume, $dxdydz$.

The heat conduction rates (perpendicular to the control surfaces of the differential volume) can be expressed in terms of qx, qy, and qz. The heat conduction rates on sides opposite the control surfaces of the control volume can be represented by a first-order Taylor series expansion, where

$$q_{i+di} = q_i + \frac{\partial q_i}{\partial i} di \qquad where\ i = x,y,z \tag{2.1}$$

In the homogeneous medium considered, an energy source may exist. This rate of thermal energy generation is denoted as

$$\dot{E}_g = \dot{q} dxdydz \tag{2.2}$$

where $\dot{q}$ is the rate of energy generation per unit volume (W/m3). Conversely, the internal energy stored by the material is

$$\dot{E}_{st} = \rho c_p \frac{\partial T}{\partial t} dxdydz \tag{2.3}$$

On a rate basis, using the principle of conservation of energy, the general form of the energy balance equation may be expressed as:

$$\dot{E}_{in} + \dot{E}_g - \dot{E}_{out} = \dot{E}_{st} \tag{2.4}$$

Combining the above equations, we obtain:

$$q_x+q_y+q_z+\dot{q}dxdydz-q_{x+dx}-q_{y+dy}-q_{z+dz} = \rho c_p \frac{\partial T}{\partial t} dxdydz$$

Simplifying, Eq. (2.4) becomes

$$-\frac{\partial q_x}{\partial x}dx-\frac{\partial q_y}{\partial y}dy-\frac{\partial q_z}{\partial z}+\dot{q}dxdydz=\rho c_p \frac{\partial T}{\partial t} dxdydz \tag{2.5}$$

Using conduction heat transfer rates postulated by Fourier's law, a phenomenological assumption, and then multiplying by the corresponding differential surface area, a heat transfer rate can be established for each coordinate direction:

$$q_x = -kdydz\frac{\partial T}{\partial x} \tag{2.6A}$$

$$q_y = -kdxdz\frac{\partial T}{\partial y} \tag{2.6B}$$

$$q_z = -kdxdy\frac{\partial T}{\partial z} \tag{2.6C}$$

Using Eq. (2.6A-C) and dividing out by the control volume, dxdydz, we obtain the heat diffusion equation:

$$\frac{\partial}{\partial x}\left(k\frac{\partial T}{\partial x}\right)+\frac{\partial}{\partial y}\left(k\frac{\partial T}{\partial y}\right)+\frac{\partial}{\partial z}\left(k\frac{\partial T}{\partial z}\right)+\dot{q}=\rho c_p \frac{\partial t}{\partial t} \tag{2.7A}$$

This is the basic equation for heat conduction analysis.

For a one-dimensional medium, in steady-state, with no

heat generation, and constant properties, Eq. (2.7A) reduces to

$$\frac{\partial^2 T}{\partial x^2} = 0 \qquad (2.7B)$$

Using boundary conditions $T_{1x=0}=T_1$ and $T_{2x=L}=T_2$, a temperature distribution can be obtained :

$$T = \frac{T_2-T_1}{L}x + T_1 \qquad (2.8)$$

Using the definition of heat flux

$$q''_x = -k\frac{\partial T}{\partial x}$$

one can obtain,

$$q'' = -k\ (T_2 - T_1)/L \qquad (2.9)$$

where q'' = heat flux

T_i = Temp. of wall surface (i=1,2)

L = wall thickness

k = thermal conductivity of material

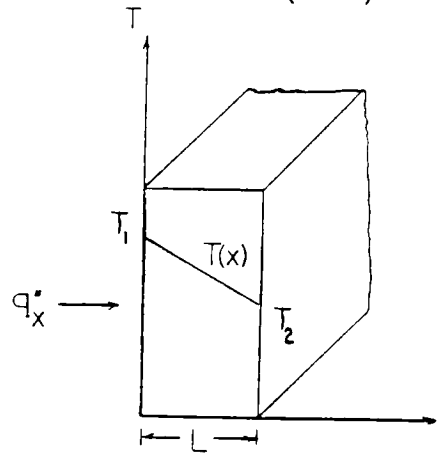

Figure 2.3
Conduction

Also, the total heat transfer rate including the wall surface area, A, can be denoted as:

$$q = q''A = -kA(T_2 - T_1)/L \qquad (2.10)$$

Convection

Convection is the mode of heat transfer that takes place between a fluid of velocity, v, and temperature, T_∞, flowing over a solid surface of arbitrary shape, as shown in Figure 2.4. If the temperature of the surface T_s is different from the temperature of the flowing fluid then heat transfer will take place by convection. The mechanism involves the transfer of energy as a result of bulk fluid motion. The rate of energy transfer is directly associated with the nature of the flow. Forced convection flow consists of moving the fluid by a external force, such as with a fan or a pump. Conversely, in free or natural convection, the fluid motion is induced by buoyancy forces resulting from a density gradient in the fluid due to the existence of a temperature difference [1].

The local heat flux is

$$q'' = h(T_s - T_\infty) \tag{2.11}$$

where h is the local convection coefficient. The total heat transfer rate when T_s is constant over the entire surface is

$$q = \int_{As} q'' \, dA_s$$
$$q = (T_s - T_\infty) \int_{As} h \, dA_s \tag{2.12}$$

The local heat transfer coefficient varies along the surface depending on many physical conditions like fluid velocity, density, temperature and surface finish. By defining an average convection

coefficient $\bar{h}$ over the entire surface, the convective heat transfer rate is:

$$q = \bar{h}A_s(T_s - T_\infty) \qquad (2.13)$$

q = heat transfer rate

$\bar{h}$ = ave. convective heat transfer coef.

T_s = surface temperature

T_∞ = fluid temperature

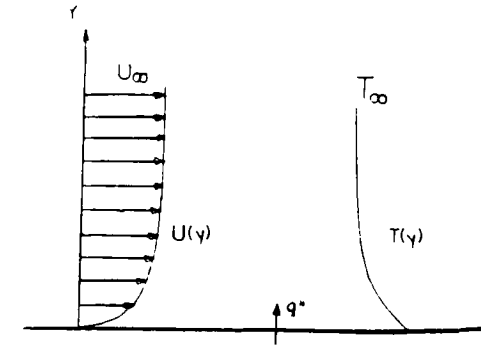

Figure 2.4
Convection

Thermal Radiation

Thermal radiation is energy emitted by matter that is at a finite temperature. The energy is transmitted through electromagnetic waves from one surface to another. The amount transmitted and/or absorbed depends upon many properties of the medium such as color, texture, and surface finish. The mechanism of radiation heat transfer is postulated by the Stefan-Boltman law,

$$q'' = \sigma \epsilon T_s^4 \qquad (2.14)$$

where,

T_s = surface temperature

σ = Stefan-Boltzman constant
(5.670E-08 W/m^2K^4)

ϵ = emissivity

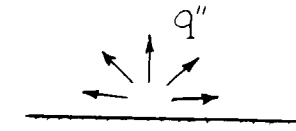

Figure 2.5
Thermal Radiation

The maximum radiation heat flux may be emitted from an ideal surface (black-body). The emissivity of a black-body is 1.0 and anything less than ideal (grey body) will be a fraction of that parameter [1].

The net radiation between two surfaces is of more practical significance. The net rate of radiation is given by

$$q_{net} = \sigma \epsilon A_s \ (T_s^4 - T_{sur}^4) \qquad (2.15)$$

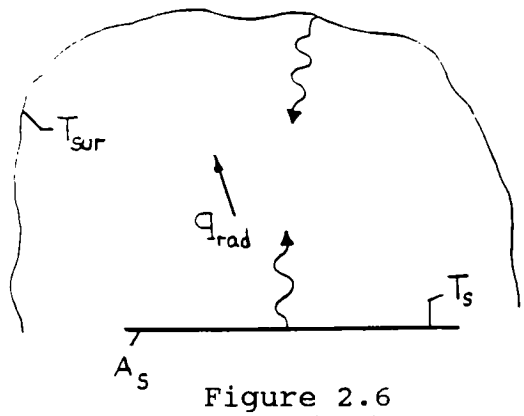

Figure 2.6
Net Radiation

where T_{sur} is the surrounding temperature and A_s is the area of the surface in question.

Although we have focused on radiation being emitted by a surface, irradiation may originate from emission or reflection occurring at other surfaces. A surface has three basic irradiation properties consisting of absorptivity, reflectivity and transmissivity.

Absorptivity is the fraction of irradiation that is absorbed by the surface and reflectivity is the fractional amount that is reflected from the surface. On the other hand, transmissivity is

associated with semi-transparent materials and is the fraction of incident radiation that is transmitted through the medium [1].

All the surface properties effects are balanced. With transparent materials, the sum total of irradiation absorbed, transmitted, and reflected equals 1.0. With opaque materials, reflectivity plus absorptivity of the incident radiation is equal to 1.0.

2.2 Heat Transfer Methods for Thin Films

Thin films are unique in nature. Their conductivities are different from the same material of a thicker gauge. Published reports have shown that the thermal conductivities of polymer films show considerable variation. This is due to a number of factors, such as molecular weights and distributions, degree of crystallinity, chain orientation, degree of cross-linking, and various content of additives.

There are established methods for determining the heat transfer characteristics of plastic based materials, exclusively in the conductive mode. Most of these methods involve contact and pressure required to lower the contact resistance between the plastic film and testing components.

Conductive testing of thin films, however, is not well established. The available techniques are usually developed for metal films. One such technique involves the use of a device called the "Thermal Comparator" [3]. This technique requires good contact

between a hemispherical testing tip and the film. This contact generally leaves an indentation on the film surface due to the creation of a high pressure point during testing.

Since some of the films tested in this study are constructed of a compressible cavitated core, which can be damaged, techniques such as the one described above can not be used. As a result, a non-contact method of determining thermal characteristics was used in this study. Also, a test at high temperatures should be avoided since the melting point of plastics is generally low.

In this study the use of a steady-state hot/cold apparatus was considered first. In order to obtain further information, a model was developed using the steady-state heat conduction equation for the temperature distribution in a hot/cold air chamber. Typical film conductivities of 0.01 to .5 W/mK were assumed along with a temperature difference of approximately 50°C (T_{hot}-T_{cold}) and film thickness of .05mm (about 2 mils).

Results from the one-dimensional model studies showed that very small temperature differences across the film are obtained, even for a film thickness of .5mm. In fact, it was determined that most materials suitable for such a steady-state hot/cold apparatus are bulk materials of at least 25 mils thick. The magnitude of films in this study range from .5 to 5 mils, most being under 2.5 mils.

Laminated stacks of film to increase the material thickness for greater testing sensitivity was also considered. But due to concern for the poor contact between films, lamination effects and

difficulty measuring small temperature differences, it was not further pursued.

The method used in this study consisted of exposing the film to a hot/cold environment as shown below :

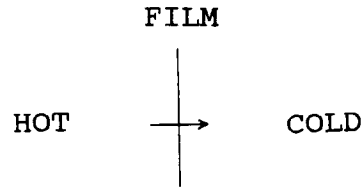

Figure 2.7

The film is subjected to a temperature differential in a convective and radiative environment.

An apparatus called an "Insulated Box" was designed and constructed from hard insulation. In testing, the box covered with film at one open side was exposed to a freezer environment and the temperature variations inside the box were recorded as a function of time.

After the successful testing of the Insulated Box, a purely conductive apparatus (Thermal Analyzer) was also designed and tested. The objective of this testing was to compare the films on a purely conductive basis. This method is similar to the technique used by Hoosung Lee [4].

The Thermal Analyzer consists of a system employing transient, one-dimensional heat transfer. Essentially, two aluminum blocks of different temperatures are at steady state at time t_o. After the two blocks are brought together with a film sandwiched between them, the resistance to heat flow is determined by measuring the temperature as a function of time in the top block.

3.0 MATERIALS & METHODS

3.1 APPARATUS AND PROCEDURES :

3.1.1 Insulated Box

In order to utilize a noncontact, transient, hot/cold apparatus, the insulated box was designed (Figure 3.1). The box was insulated with two inch rigid insulation on five sides. The top side was left open for fitting the film sample. Three thermocouples were equally suspended inside the box along its vertical depth. One thermocouple was placed very close to the film without touching it and another at the bottom of the box.

The thermocouple at the bottom served two purposes: first, to determine when the inside of the box had reached steady-state, and second, to qualify that the transmission of heat through the rigid insulation was minimal compared to the transmission through the top side. The top of the box was fitted with a thin plexiglass plate to secure films with an adhesive spray glue.

The box with constant temperature air inside was fitted with the film and placed film side down (to minimize natural convective effects) inside a freezer approximately at -30° C. The freezer controls were bypassed to enable the freezer to operate continuously and reach a steady, maximum, cold potential.

Thermal transmission takes place from the box, through the film and into the freezer. Temperature, as a function of time, was recorded until the air inside the box reached the stable freezer temperature. The freezer temperature adjacent to the film surface

was also recorded. The actual response was determined using the dimensionless parameter:

$$(T_1(t) - T_\infty)/(T_1(0) - T_\infty)$$

The response of the dimensionless parameter vs. time was plotted for each film. Repeated testing showed good reproducibility of the data.

The Insulated Box was also used in a series of separate tests using automobile antifreeze as the internal fluid. The use of a liquid in the box eliminated any interior radiation effects that may be present.

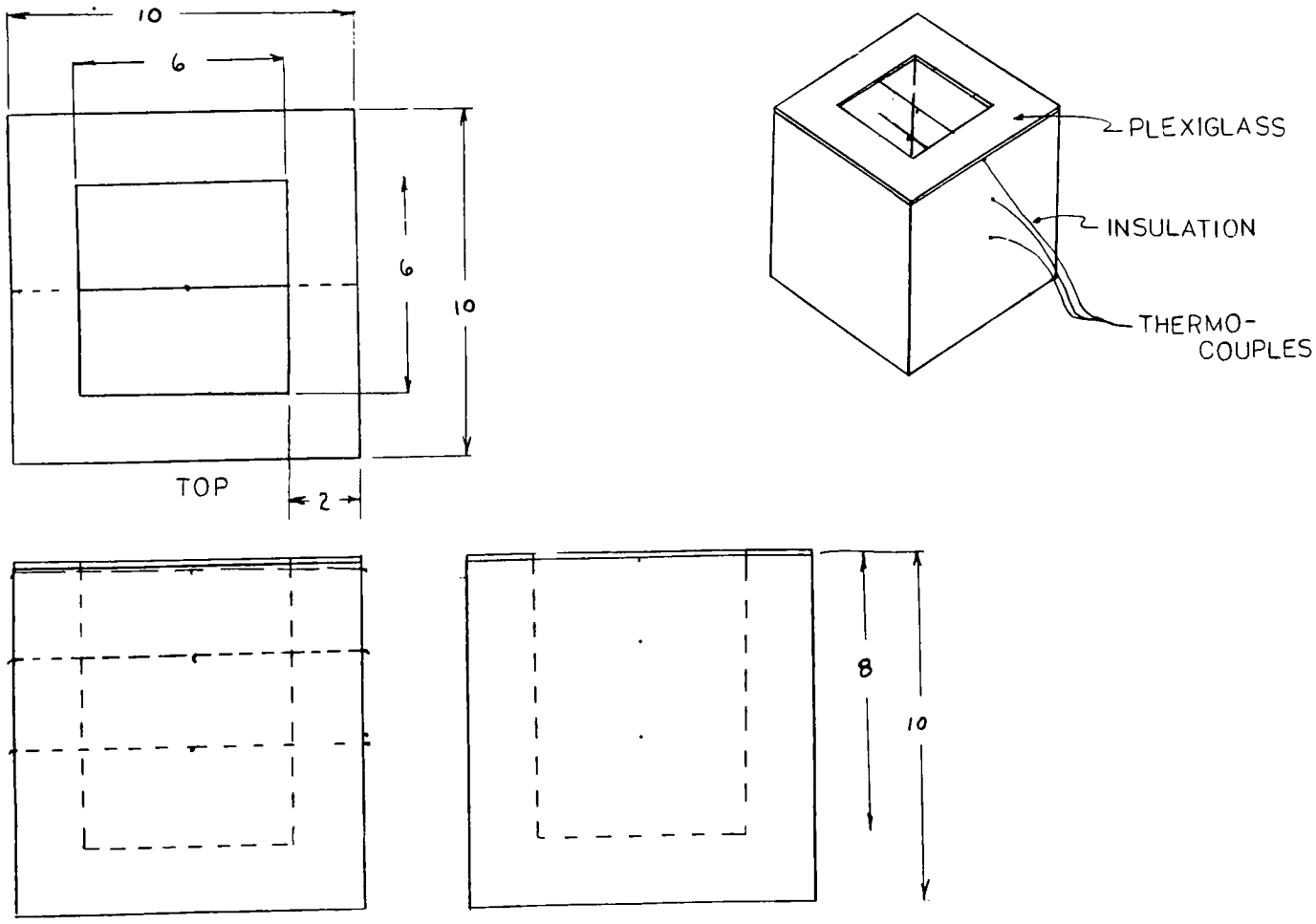

Figure 3.1
Insulated box

3.1.2 Thermal Analyzer

Using the Hoosung Lee [4] approach, the Thermal Analyzer which is schematically shown below, was designed.

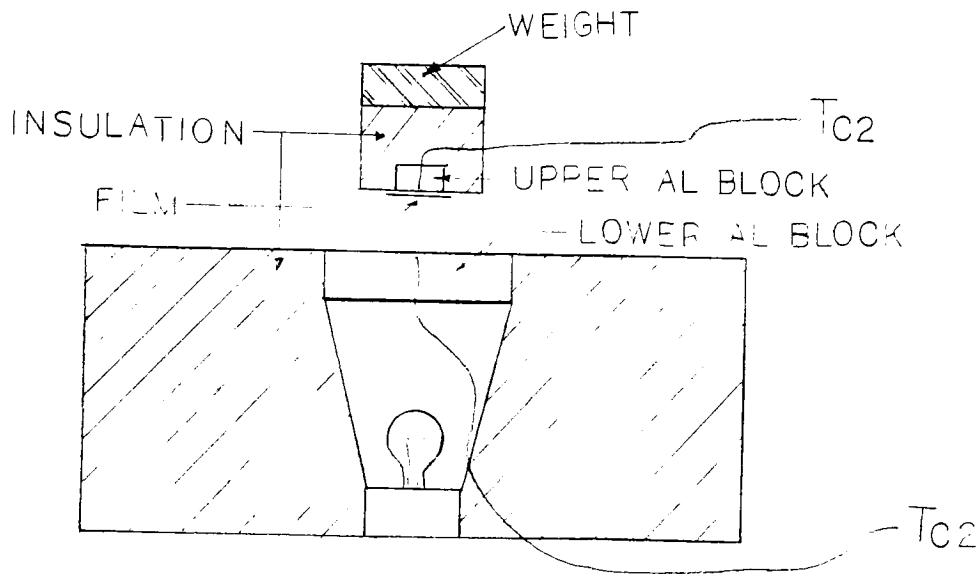

Figure 3.2
Thermal Analyzer

The actual test apparatus includes a two block system with the lower block maintained at a constant temperature and the upper block being in transient response. Both blocks are surrounded by rigid insulation in order to eliminate heat transfer from the sides. Therefore, the primary energy transmission is one-dimensional. The lower block is kept at a constant temperature of 60°C by a heat source consisting of a microscope lamp. The top block was initially at room temperature of about 20°C. Two

thermocouples were mounted in the blind holes as close to the block surfaces as possible.

A single film sample was placed onto the top block with a small amount of high vacuum silicon grease to reduce the contact resistance between the two mediums. A small amount of weight was applied to the top block to provide some pressure for good contact. Tests were performed using identical films to ensure this weight provided good repeatable responses. The thermocouple mounted in the bottom aluminum block remained constant throughout testing.

When the blocks were brought in contact, the temperature was measured as a function of time, until the thermocouple 1 (upper block) reached the equilibrium temperature of 60° C. Consecutive tests were completed with each film for reliability. Once again, the dimensionless parameter

$$(T_{tc1}(t) - T_{tc2})/(T_{tc1}(0) - T_{tc2})$$

was used for recording the thermocouple responses. Good reproducibilty was obtained.

4.0 RESULTS AND DISCUSSION

4.1 Insulated Box

All of the films listed in Table 4.1 were tested with the Insulated Box. The results are organized by the following classification: cavitated OPPalytes, coextruded oriented polypropylene, metallized, OPPalyte/metallized and conventional.

OPPalytes vs. Coextruded Oriented Polypropylene

The transient response are shown in Figure 4.1. The comparisons show that there is no difference between the responses. For individual or film composite between 1.0 to 2.0 mils, film gauge, opacity, or composite makeup have no significance.

Metallized vs. Non-metallized OPPalytes

The results of these tests are shown in Figure 4.2. Aluminum foil and metallized films show a greater insulative barrier than nonmetallized films (OPPalytes, coextruded oriented polypropylene, or polyethelene). This is indicated by the slower temperature drop as a function of time.

Metallized/OPPalyte

The results from these tests are also shown in Figure 4.2. Tests were performed with different film positioning as well. "In" denotes the metal side facing inside the box (facing warm air); whereas, "out" denotes the metal facing out towards the cold

environment. The results showed that the insulative protection depended upon film surface positioning. In comparison, when the metallized side faced in (ie. warm side), it was less insulative than when the metallized side faced out (cold space).

Metallized/OPPalyte vs. all others

The metallized/OPPalyte films were compared to aluminum foil and nonmetallized films. These results are also shown in Figure 4.2. It is observed that aluminum foil and metallized/OPPalyte with metallized facing "out" have essentially the same response. Although metallized/OPPalyte faced "in" (towards warm space) was less insulative than aluminum foil or metallized facing "out", it was still more insulative than any other nonmetallized films.

Conventional films vs. all others

The conventional films responded correspondingly to the other films of similar structure as shown in Figure 4.3. The transient response of aluminum foil was very similar as metallized films. Waxed paper and freezer paper responded like polymer films. Also, foil/paper responded the same as metal/polymer composite films.

Box Filled with Antifreeze

The transient response of the box filled with antifreeze is much slower than the box filled with air as shown in Figure 4.4. Aluminum foil is also more insulative than polyethelyne in this scenario, repeating the results of the air filled box.

Figure 4.1 Freeze cycles of 1.0 mil coex OPP/1.0 mil coex OPP, 1.0 mil coex OPP, 1.1 mil coated OPPalyte/.75 mil cellophane.

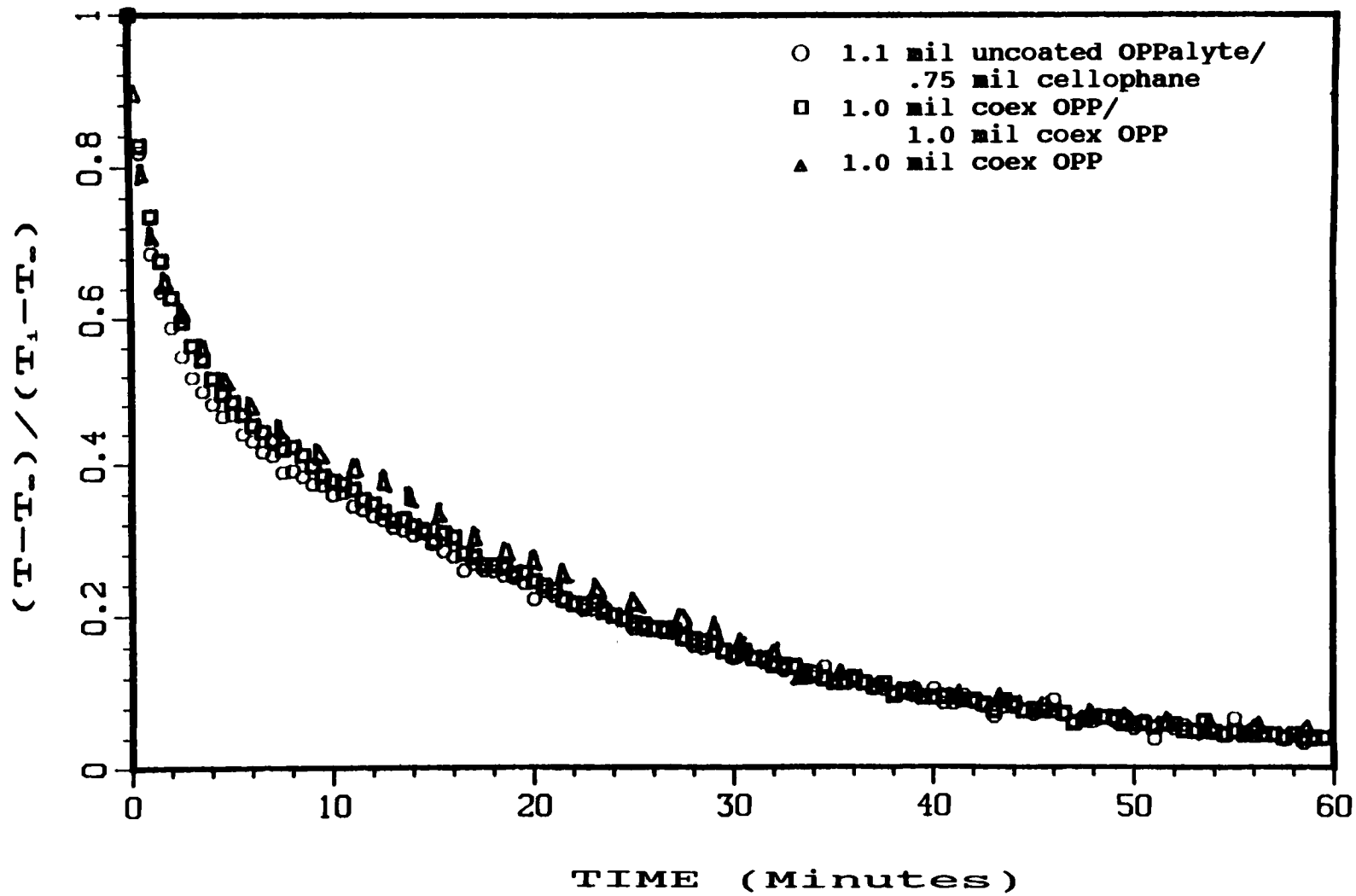

T_∞ = Freezer Temp.
T_i = Initial Box Temp.
T = Temp. adjacent to film

Figure 4.2 Freeze cycles of aluminum foil, white pigmented polyethlene, 1.5 mil uncoated OPPalyte, and metallized 1.5 mil uncoated OPPalyte.

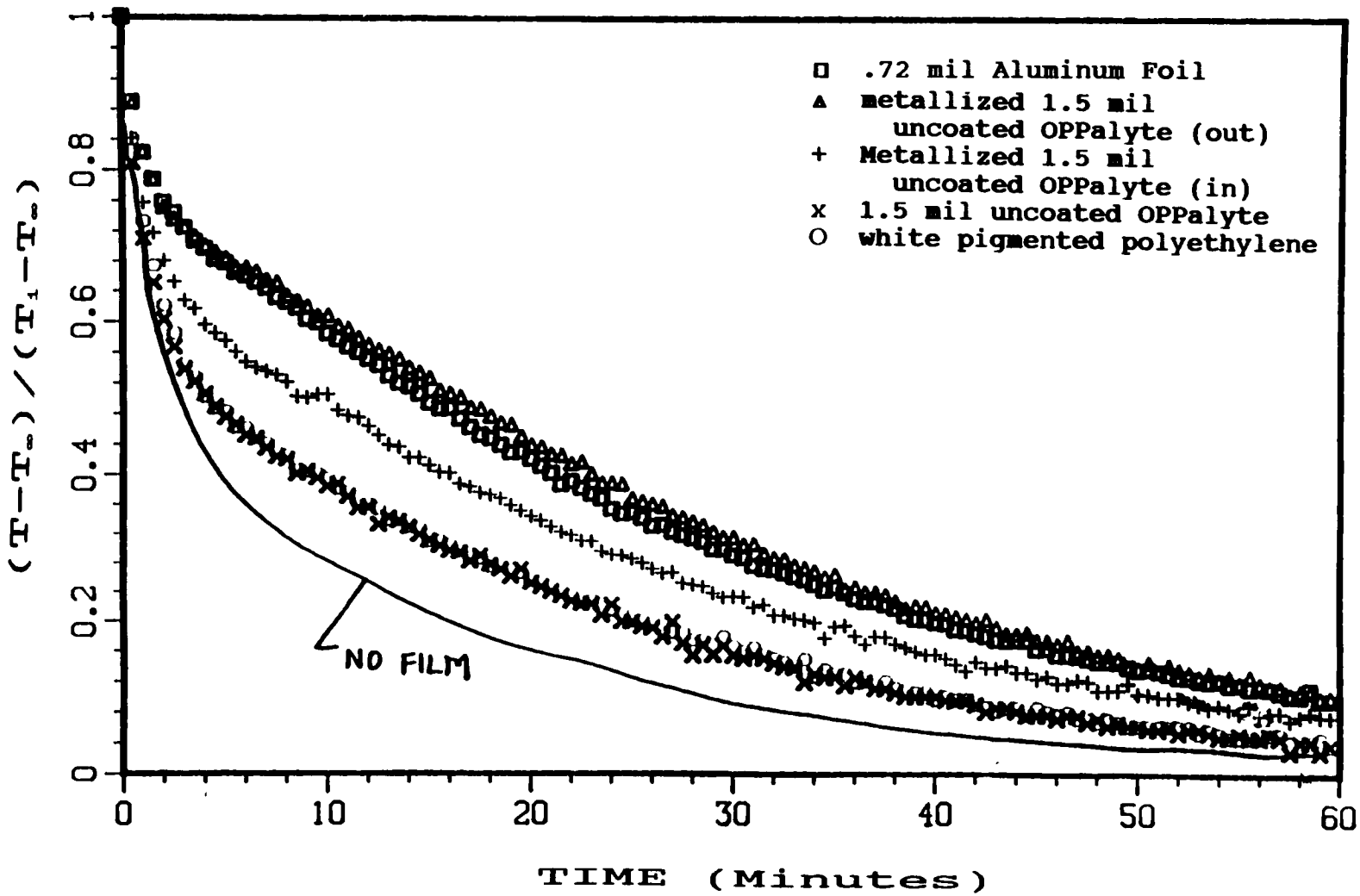

T_∞ = Freezer Temp.
T_i = Initial Box Temp.
T = Temp. adjacent to film

Figure 4.3 Freeze Cycles of aluminum foil, 1.4 mil Metallyte, wax paper, and 1.4 mil uncoated OPPalyte.

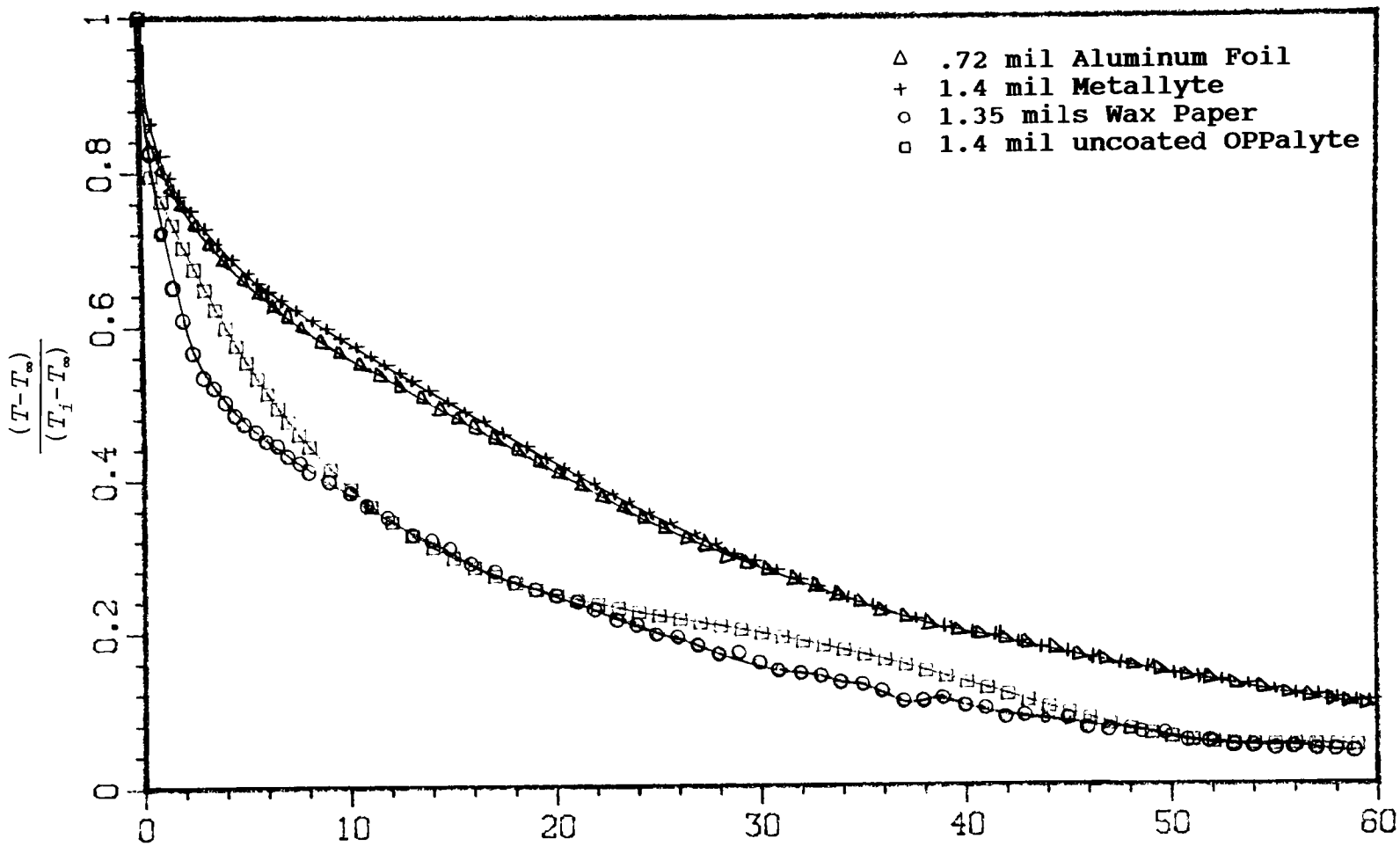

T_∞ = Freezer Temp.
T_i = Initial Box Temp.
T = Temp. adjacent to film

Figure 4.4 Freeze cycles with Insulated Box filled with antifreeze and air. 1.5 mil Polyethelyne vs. .72 mil Aluminum Foil

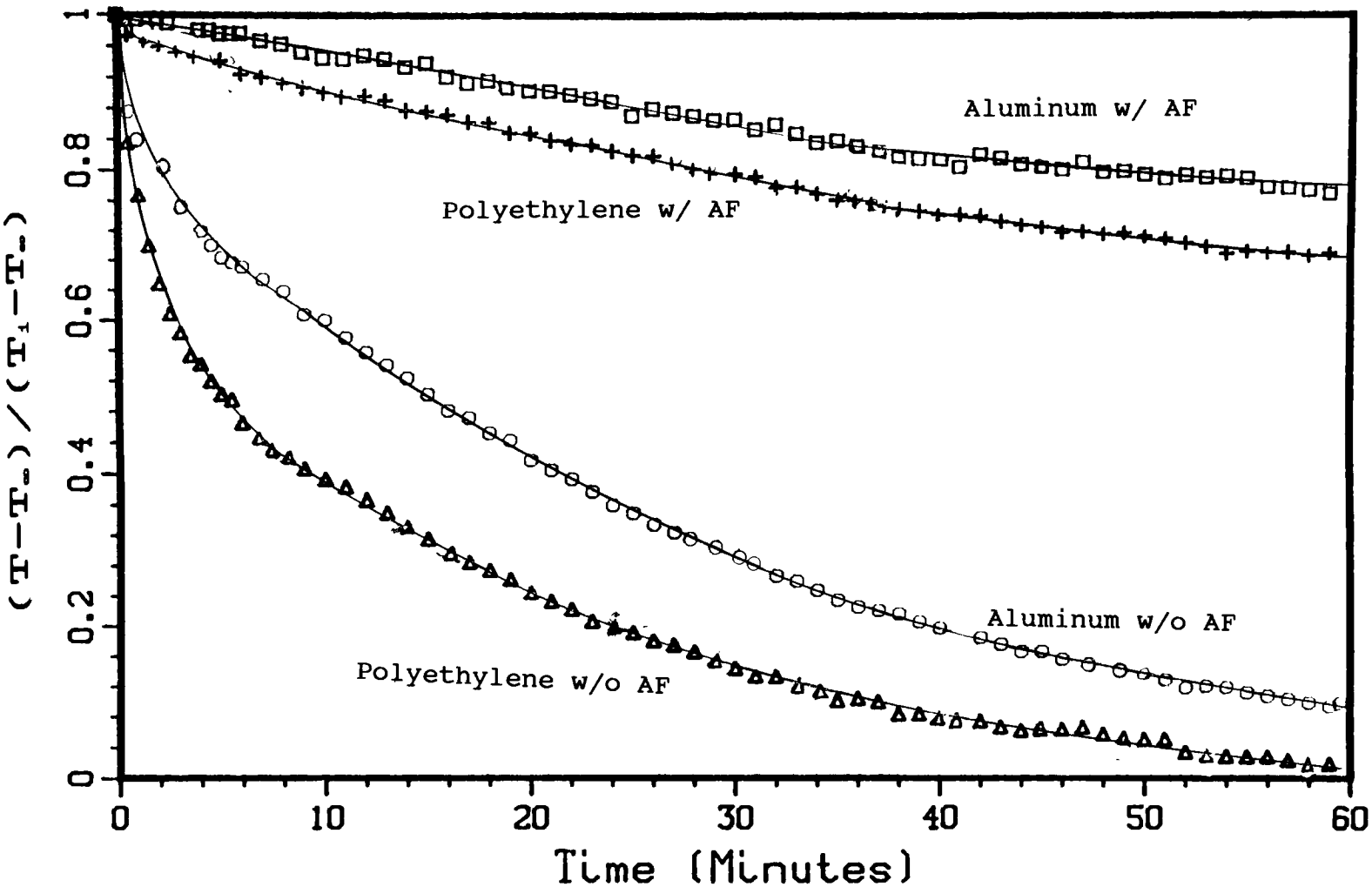

T_∞ = Freezer Temp.
T_1 = Initial Box Temp.
T = Temp. adjacent to film

Discussion of Results

The general trend of results can be attributed to radiation properties of the film, specifically emissivity. The insulated box results emulate the governing equation of net radiation transfer between two surfaces and free convection between two surfaces and surounding air. The convection coefficient, h (W/mK), is held moderately constant in the test procedure. Thus, depending on the given emissivity of the film, surface finish and surrounding temperatures, the heat transfer rate through the film will be slower or faster.

Highly polished aluminum surfaces have a very low emissivity (approximately .05) and high reflectivity; whereas, white or clear plastic films have an emissivity of about .9 . The low emissivity of polished aluminum allows for minimal radiation to take place between the inside and outside film surfaces and its surroundings, making it an insulative material under these conditions when compared to polymer films.

When nonmetallized films are used, the absorbed radiation energy from the inside of the box is transmitted more easily to the freezer environment due to high emissivity.

Metallized composite films with the metallized surface "out" (metal facing cold) are more insulative than those with the metallized surface "in" (metal facing warm). The low emmisivity on the outside surface contributes to low thermal transmission.

The dominant surface radiation must take place between the

outside of the film and the freezer environment, since both aluminum foil and metallized composite films with the metallized surface "out" have very close responses.

For metallized composite films with metallized surface "in" (metal facing warm), the transmissivity is zero causing the film to be more insulative than the nonmetallized opaque films, but the nonmetal surface facing toward the cold space radiates more energy making the film less insulative than with the metallized surface "out".

Effective use of these results can be summarized in the following manner:

APPLICATION	SURFACE POSITIONING	
	METALLIZED SURFACE	PLASTIC SURFACE
Quick Freeze	Facing Warm Space	Facing Cold Space
Slow Freeze	Facing Cold Space	Facing Warm Space
Quick Thaw	Facing Cold Space	Facing Warm Space
Slow Thaw	Facing Warm Space	Facing Cold Space

As noticed, depending on the manufacturer's needs and applications, one can benefit from the use of the films radiative properties.

4.2 Thermal Analyzer

The Thermal Analyzer, on the other hand, was experimentally set-up as purely a one-dimensional, transient conduction apparatus. This method utilizes a few factors essential for thin film heat transfer measurements:

1) Quick transient transmission of heat (about 60 seconds for most films to reach equilibrium).
2) A conducting medium (aluminum) that has a significant magnitude of difference in properties to plastic films.
3) A well insulated set-up to minimize convection and radiation effects.

The results from Thermal Analyzer testing were reproducible. The weights on top of the upper block produced good contact and reliable data with no apparent damage to the film. The weight distributed over the film surface was considered to be on the same order of magnitude as in packaging applications. A few different films were initially tested to ensure good reliability of the Thermal Analyzer results. The initial testing provided a ±5% tolerance in consecutive test runs.

The results from the films tested with this method are shown in the transient responses of dimensionless temperature and also in Table 5.1 which also lists gauge, and apparent conductivity (discussed in next section).

The Thermal Analyzer results are organized in the following groups: metallized, coextruded oriented polypropylene, cavitated OPPalytes, OPPalyte/metal composite and other conventional films

along with film gauge.

Metallized Films

The metallized films are less insulative when compared to cavitated films, see Figure 4.5.

Film Gauge

The films become more insulative with increasing thickness. See Figures 4.6 and 4.7. The apparent conductivity (Discussed in section 5.3) of a particular film type is not necessarily the same with varying thickness. This is due to the the composite structure of the film. The ratio of the core thickness to other layers may not be equivalent in each film type.

MATERIAL	Measured Gauge (mils)	K(apparent) (W/mK)
Group 1 (Cavitated Core Films)		
1.40 mil uncoated OPPalyte	1.27	.022
2.00 mil uncoated OPPalyte	1.61	.0235
2.50 mil uncoated OPPalyte	2.34	.0225
Group 2 (Cavitated Core Films)		
1.60 mil coated OPPalyte	1.59	.0275
1.50 mil coated OPPalyte	1.34	.024
Group 3 (Solid Films)		
1.40 mil coex. oriented polypropylene	1.42	.040
1.00 mil coex. oriented polypropylene	.98	.032
.80 mil coex. oriented polypropylene	.79	.037

Table 4.1

Figure 4.5 Thermal Analyzer results showing metallized vs. OPPalytes and non-OPPalytes.

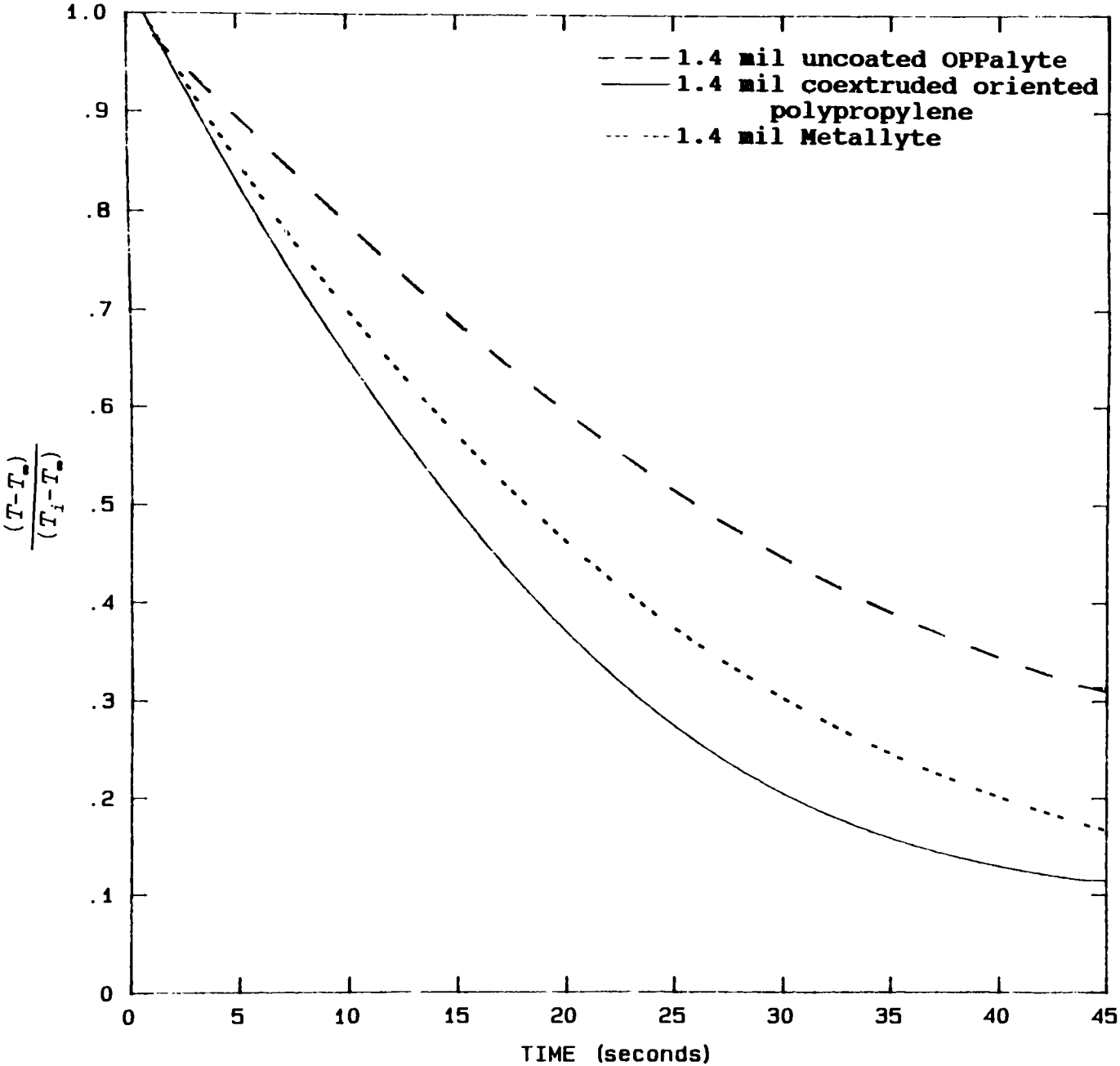

Ti = Temp at thermocouple 1 initially
T∞ = Temp of constant lower block

Figure 4.6 Thermal Analyzer results showing the effect of gauge for uncoated OPPalyte.

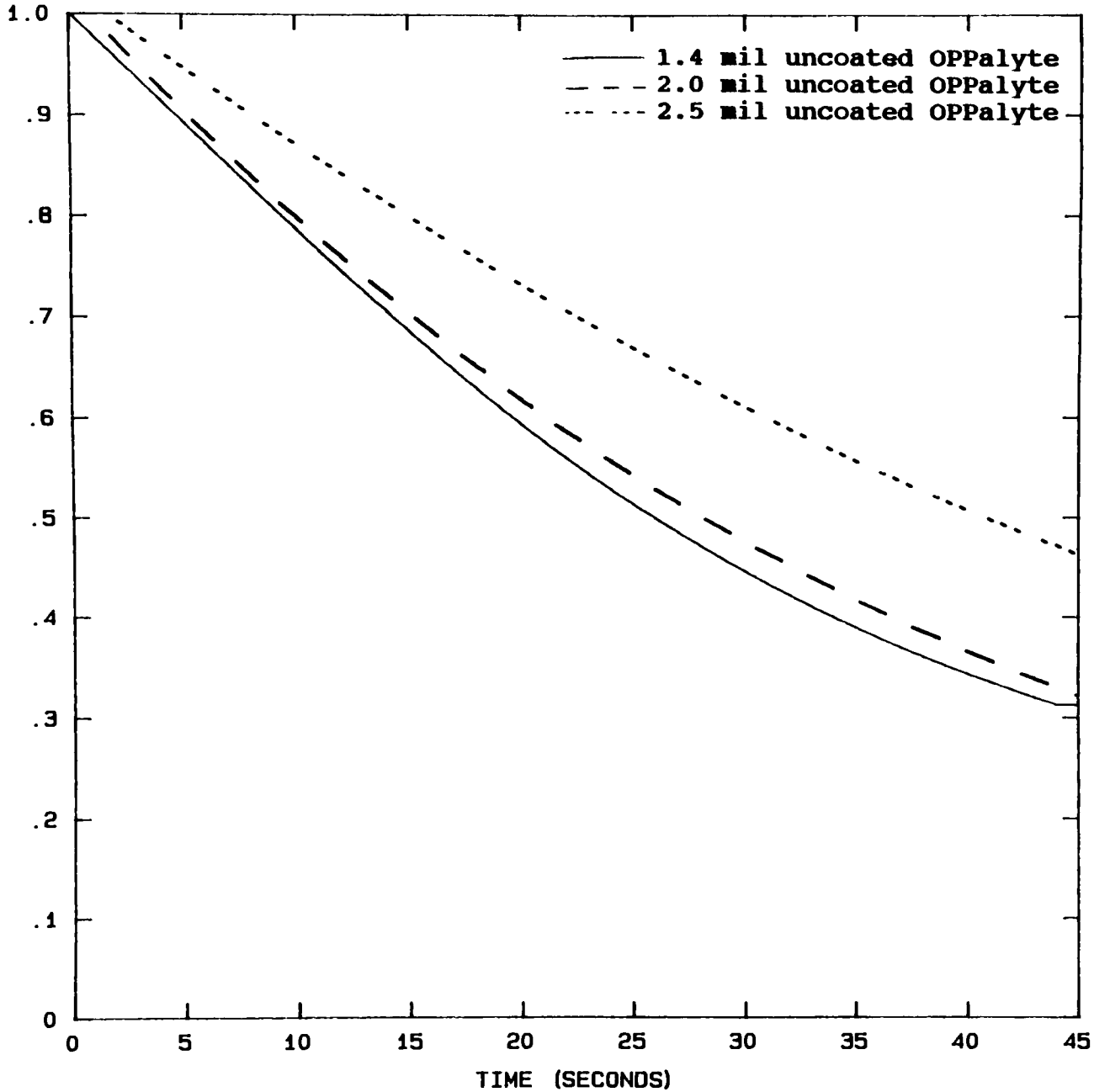

Ti = Temp at thermocouple 1 initially
T∞ = Temp of constant lower block

Figure 4.7 Thermal Analyzer results showing the effect of gauge for coextruded oriented polypropylene (OPP).

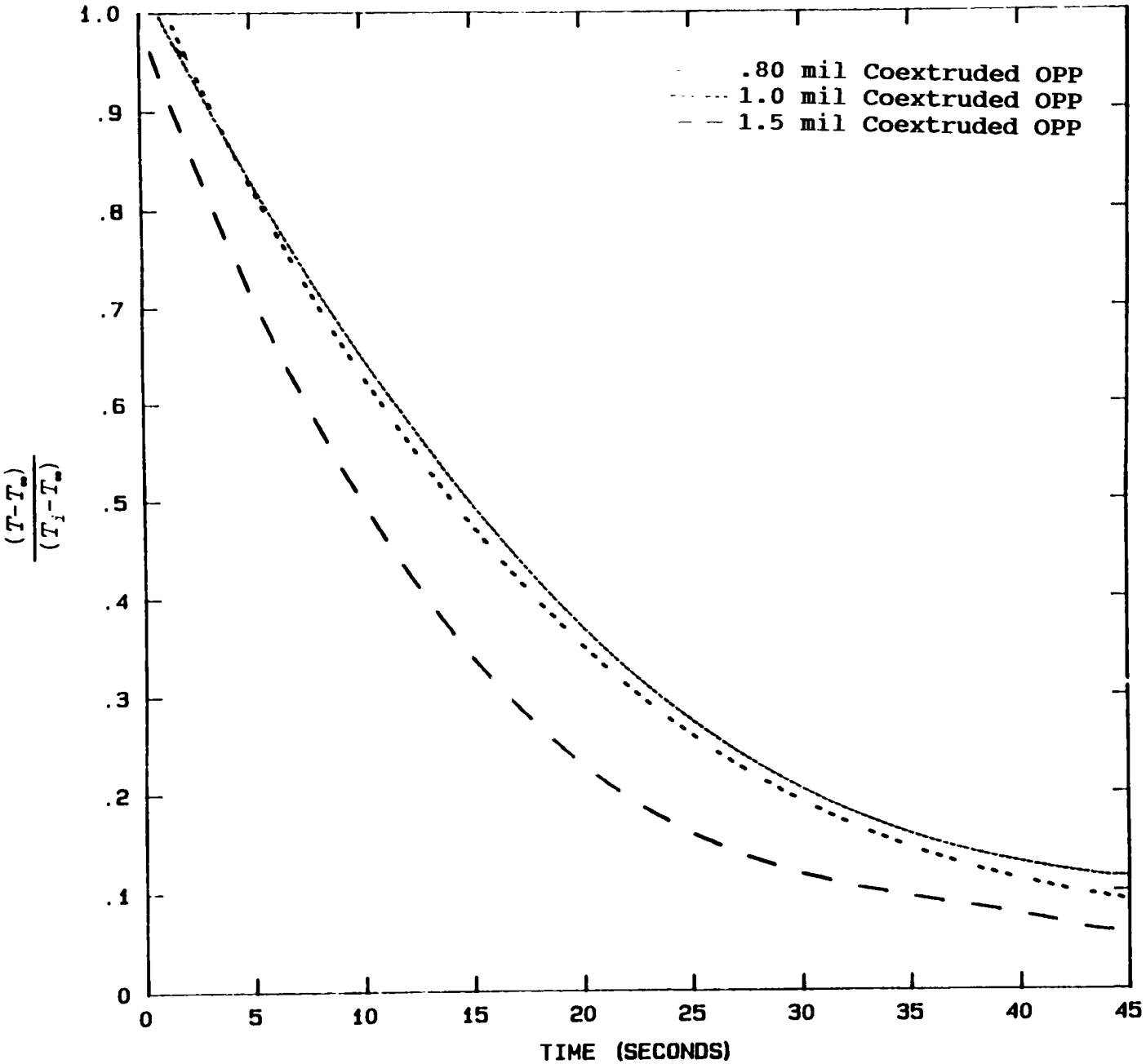

Ti = Temp at thermocouple 1 initially
T∞ = Temp of constant lower block

OPPalyte vs. Coextruded Oriented Polypropylene

The cavitated cores in OPPalyte films produce a thermal barrier better than solid films; consequently, their conductivities (See Table 4.1) are lower. Also, see Figure 4.8.

Metallized/OPPalyte

The results show very small difference between the metallized/OPPalyte and the plain OPPalyte films. See Figure 4.9.

Conventional films

Conventional films such as polyethylene and paper products are not as insulative as OPPalytes. This is due to the thinner gauge and the absence of a cavitated core.

Other results than those referred to here can be seen in the Appendix 7.3.

Figure 4.8 Thermal Analyzer results showing OPPalytes vs. non-OPPalytes.

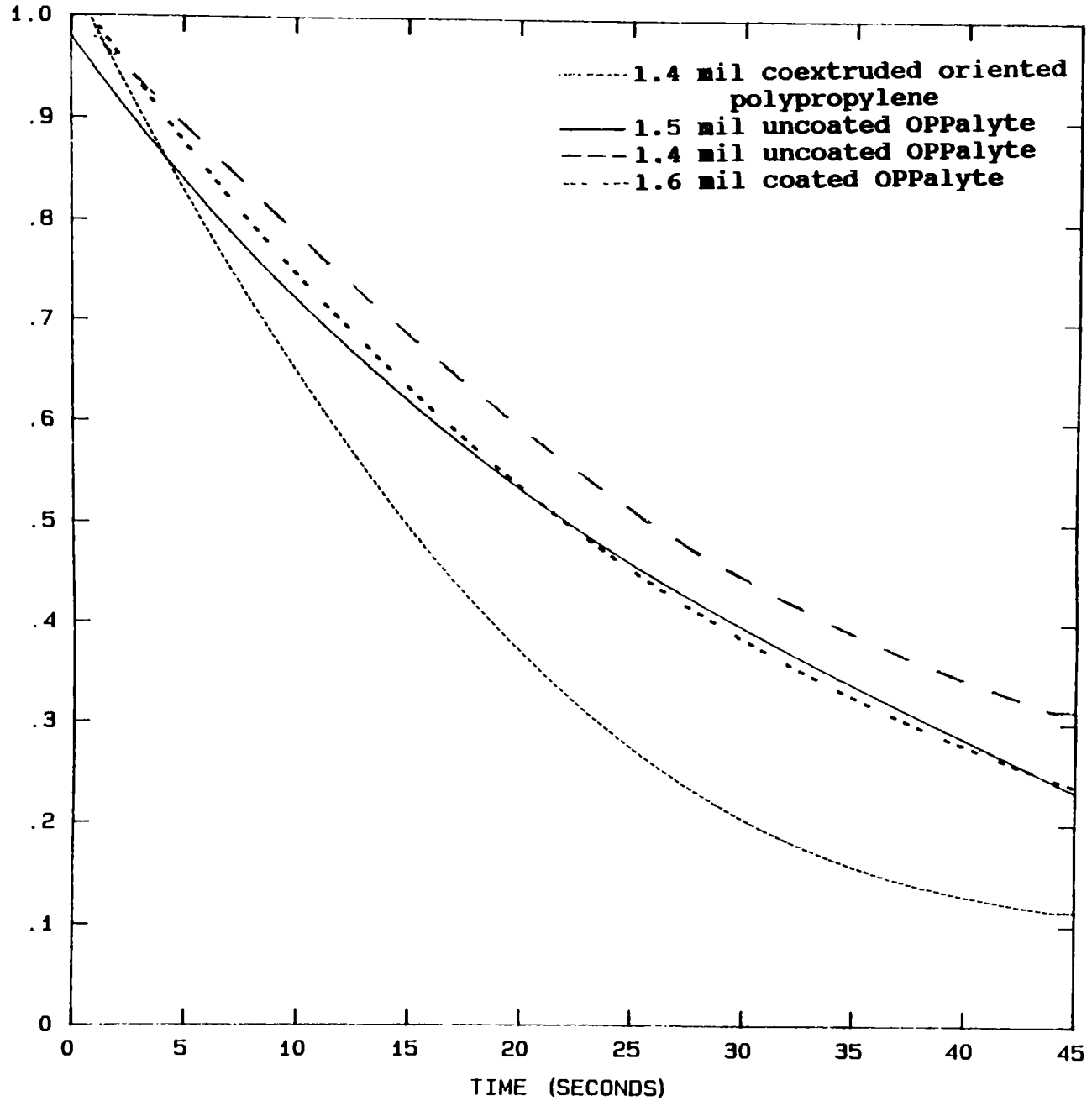

Ti = Temp at thermocouple 1 initially
T∞ = Temp of constant lower block

Figure 4.9 Thermal Analyzer results showing metallized vs. nonmetallized 1.50 mil uncoated OPPalyte.

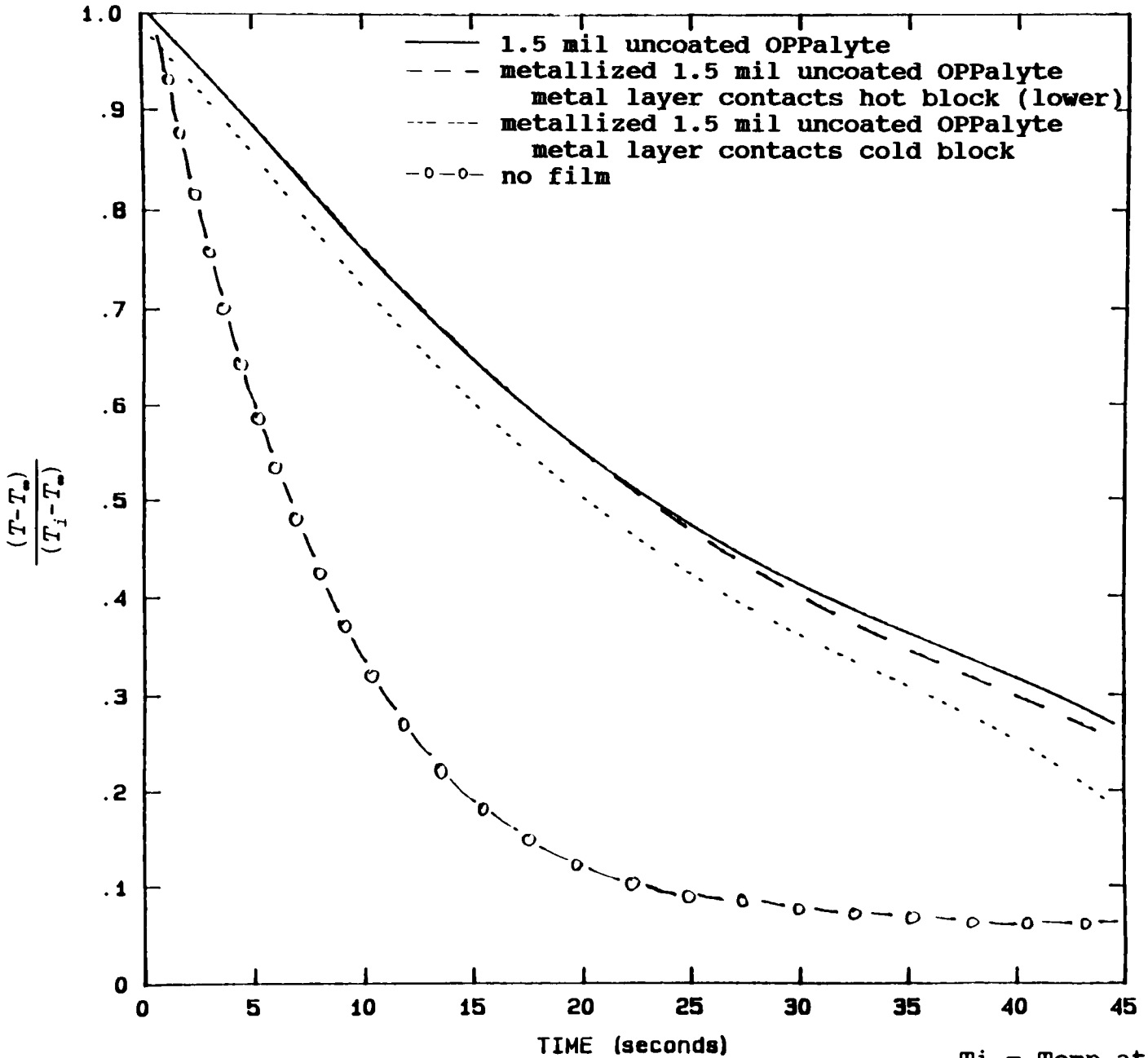

Ti = Temp at thermocouple 1 initially
T∞ = Temp of constant lower block

4.3 Statistical Analysis

The Insulated Box and the Thermal Analyzer were analyzed for confidence to establish significance in the differences seen in the transient responses.

First, the Insulated Box data was grouped according to film type: nonmetallized, metallized, nonmetallized/metallized composite facing "in" and facing "out". The groups of data were run through the SAS statistical package for a 95% confidence interval (tolerance bars) of the cubic line fit used to estimate the dynamic response.

Results showed that the groupings of data (ie. nonmetallized) have statistically significant differences, just as first assumed. The 95% confidence interval bars are drawn about the cubic estimation in Figure 4.10. The tolerance bars ranged from ∓0.02 (dimensionless quantity) at the beginning and end of the response to ∓0.01 at about 30 minutes into the test run.

The Thermal Analyzer data was grouped using 3 to 4 experimental test runs of each individual film. These data groups were statistically analyzed using SAS to find 95% confidence interval on the cubic line estimation of the dynamic responses.

The results showed a maximum of ∓0.01 tolerance (dimensionless quantity) for each film response. See Figures 4.11 through 4.14. This data shows good reliability in the test method and a high level of confidence in the differences established between the films.

Figure 4.10 95% Confidence Interval Bars on Insulated Box Results

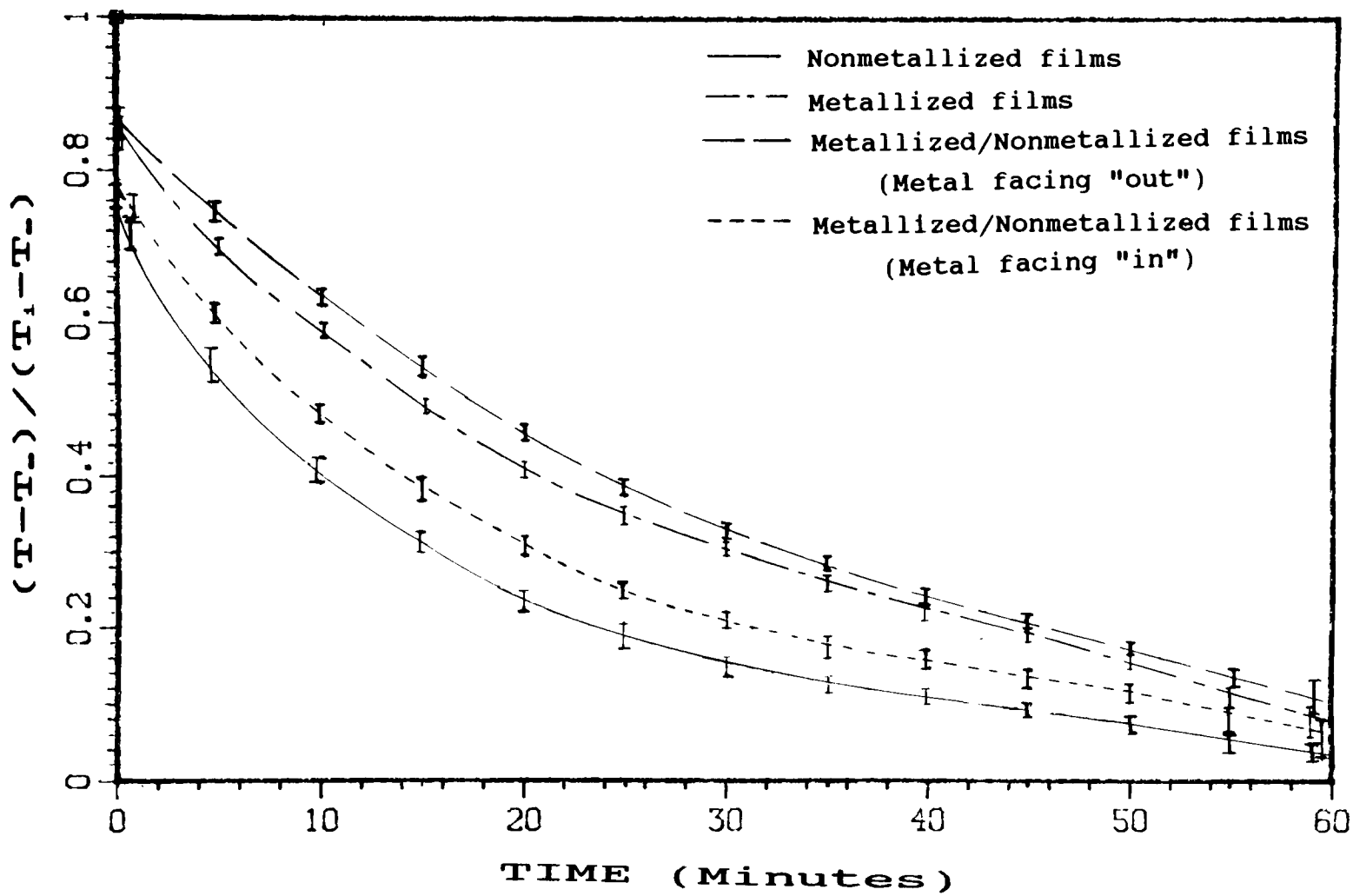

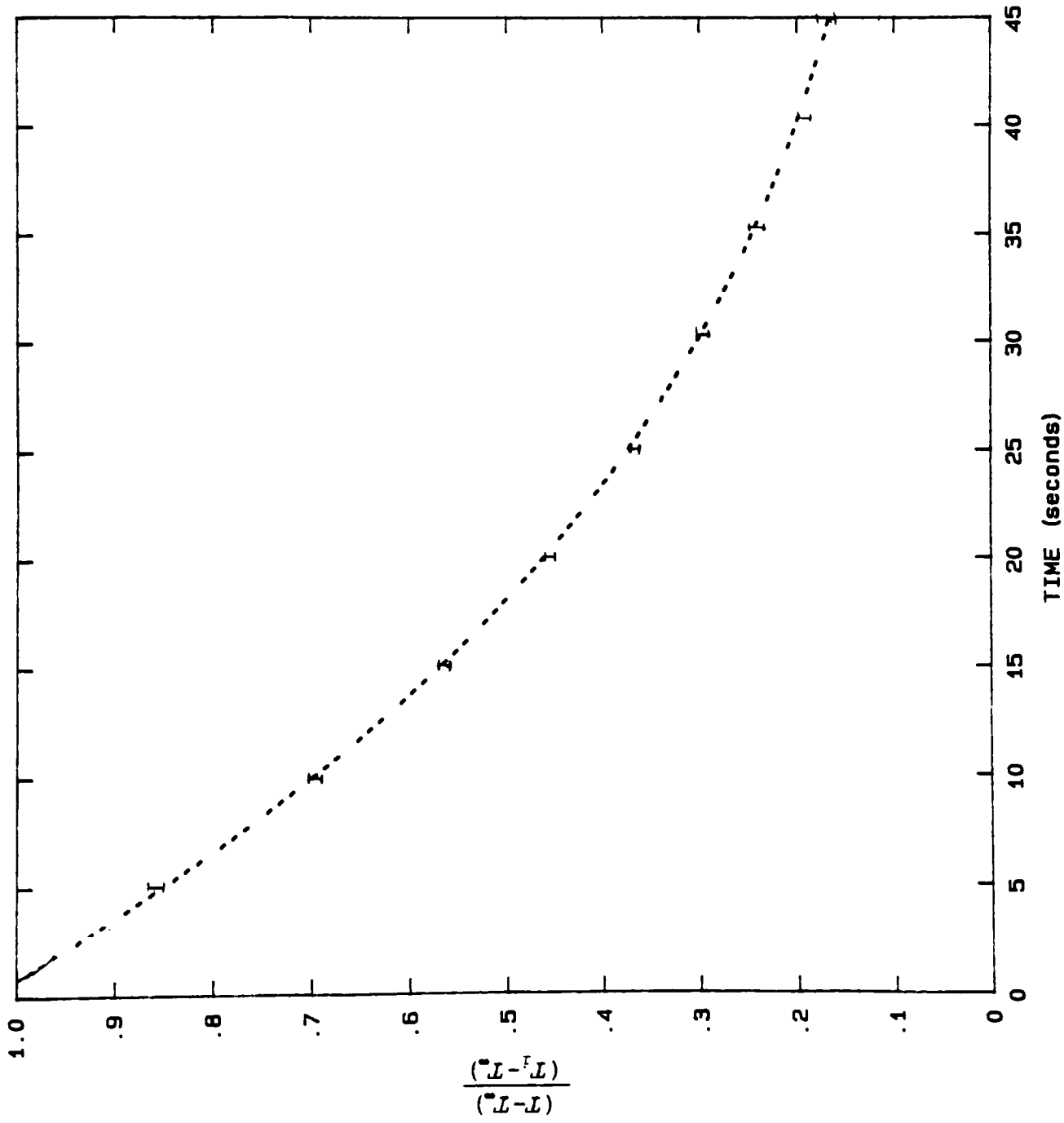

Figure 4.11 Thermal Analyzer Results of 1.40 mil Metallyte w/ 95% Confidence Interval Bars

Figure 4.12 Thermal Analyzer Results of 1.40 mil Coextruded Oriented Polypropylene w/ 95% Confidence Inetrval Bars

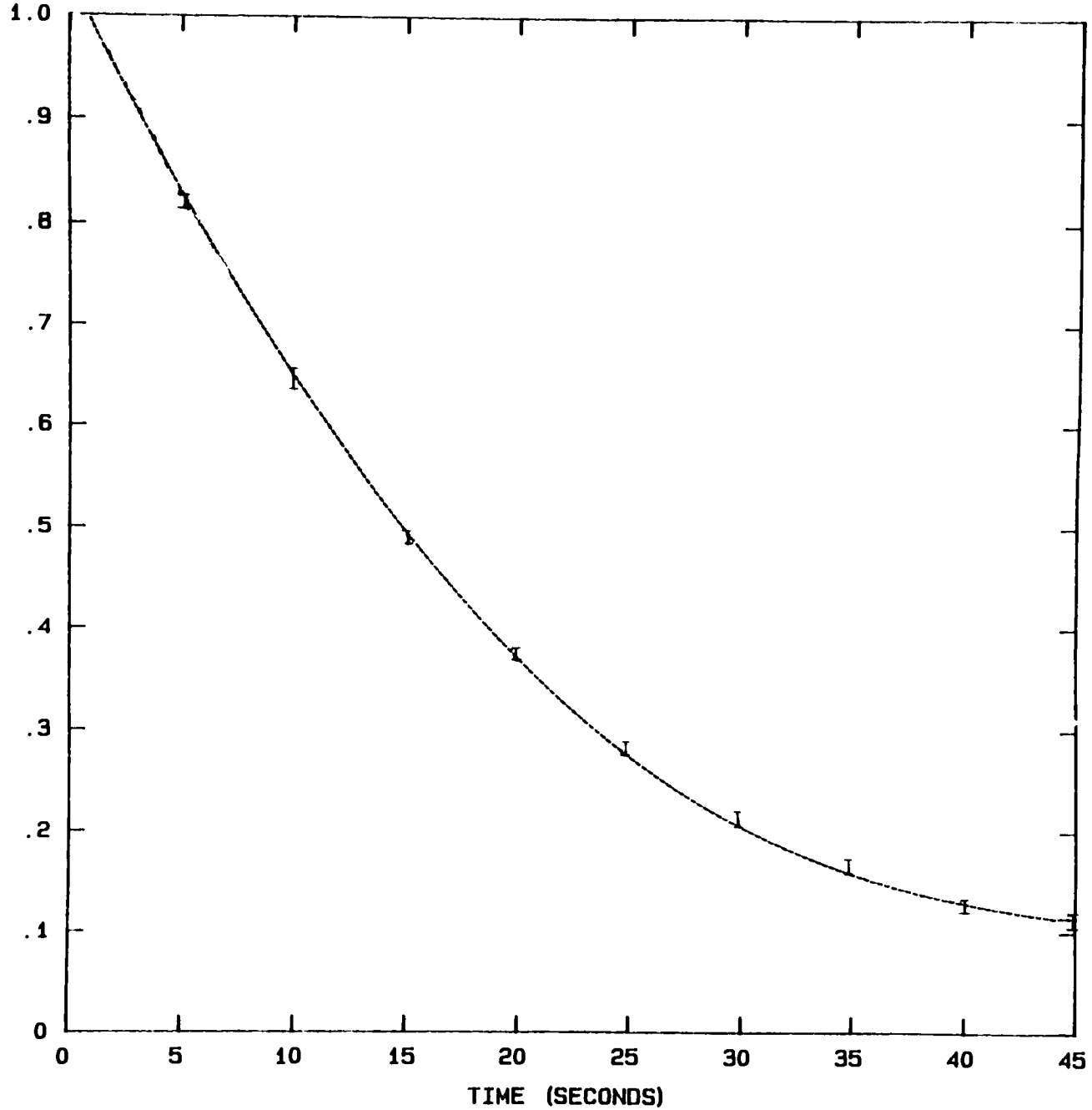

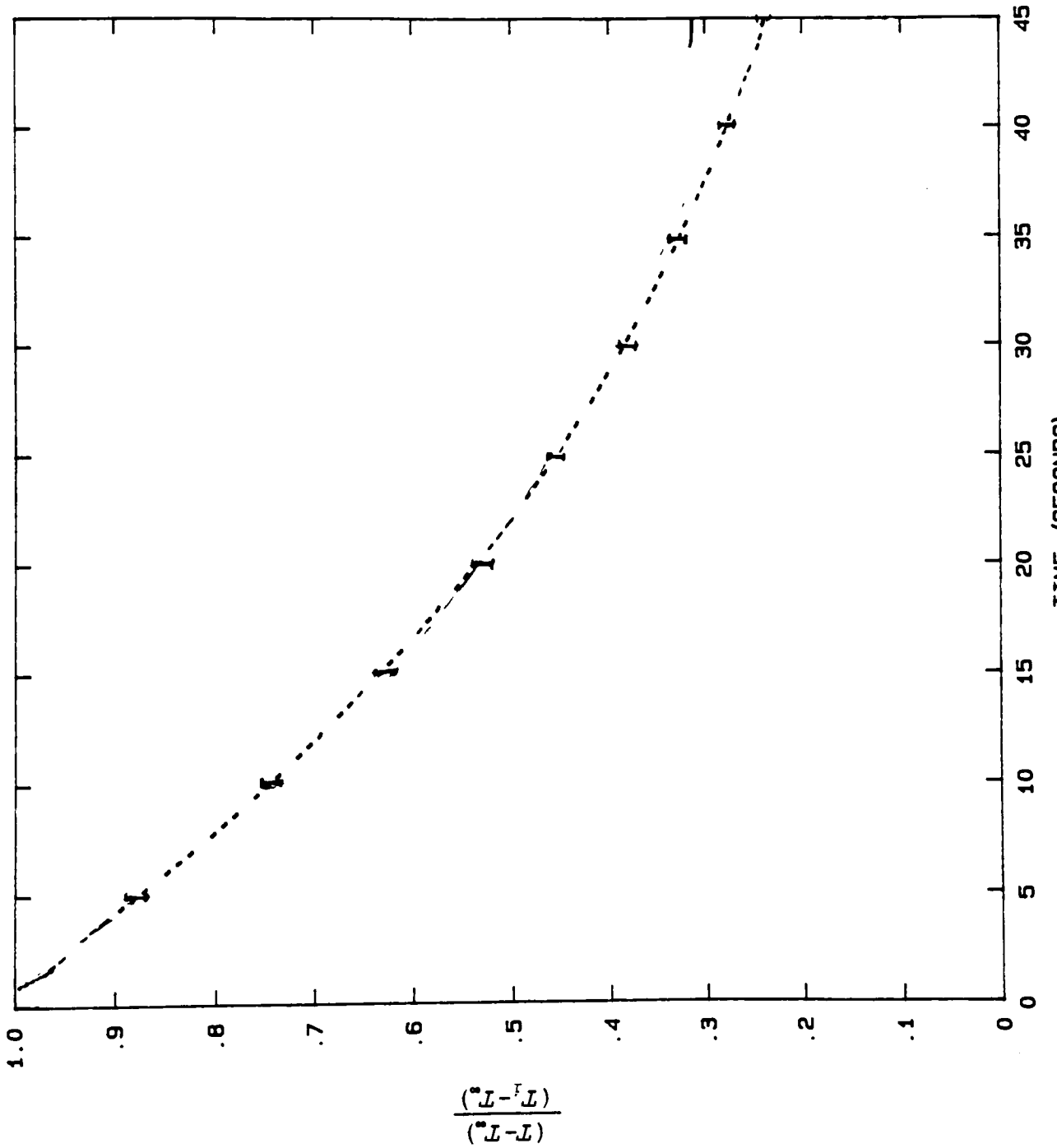

Figure 4.13 Thermal Analyzer Results of 1.50 mil Coated OPPalyte w/ 95% Confidence Interval Bars

Figure 4.14 Thermal Analyzer Results of 1.77 mil High Opacity Sealable White Opaque w/ 95% Confidence Interval Bars

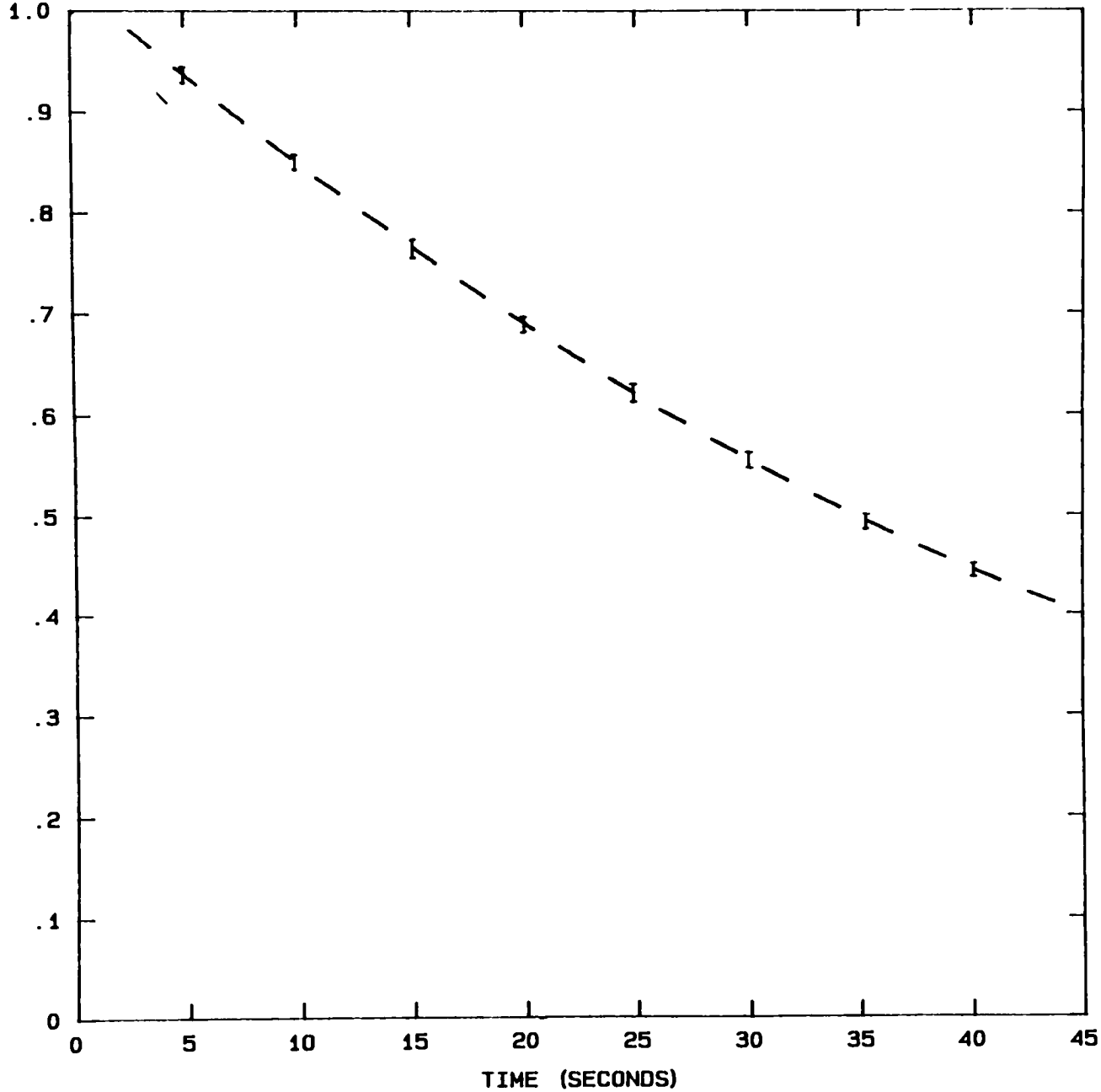

5.0 MODELING And SIMULATION

5.1 INSULATED BOX

The insulated box was analytically modeled to verify the dominance of radiation heat transfer over the convection mode, as well as to assess the relative effect of film emissivity. The model was motivated by the radiation effects detected experimentally.

The first-order model is based on a lumped capacitance medium consisting of a fluid in a insulated box that can only transmit heat through a film on one open side (see Figure 5.1).

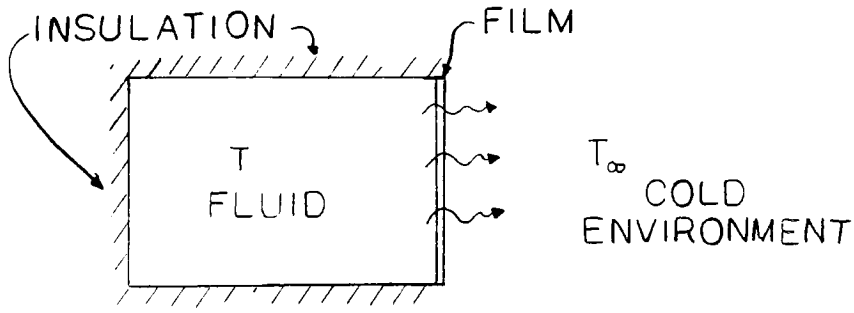

Figure 5.1

When investigating the combined effects of radiation and convection in this one-dimensional model, certain assumptions must be established. First, the fluid/film inside the box will be lumped as a uniform body of matter that has a given capacitance of heat. Also, the properties of the fluid are assumed to be constant

throughout the process.

The first-order differential equation governing the heat transfer across the film is deduced from energy considerations as:

$$\rho\, C\, v\, dT/dt = -[\, h\, A\, (T_1 - T_\infty) + \epsilon A \sigma\, (T_1^4 - T^4_\infty)\,] \qquad (5.1)$$

(heat flux) = (convective term) + (radiative term)

in which :

ρ = density (combined)
C = Specific Heat (combined)
V = volume
T = Temperature of the body
h = convection coefficient
A = film surface area
T_∞ = ambient surface temperature
ϵ = surface emissivity
σ = Stefan-Boltzmann constant
T_1 = Temperature of thermocouple 1

The values of the constants in Eq. (5.1) were extracted from insulated box measurements and convection assumptions as:

$V = .00375\ m^3$	$A = .022\ m^2$
$h = 10\ W/mK$	$T_\infty = -30^\circ C$
$0. \leq \epsilon \leq 1$	$\sigma = 5.67 * 10^{-8}\ W/m^2K^4$

Two simulations were performed to qualitatively model the experimental results.

Case 1 : Air filled box

$\rho_{comb} = 1.0\ kg/m^3$, C = 1007. J/kgK

Case 2 : Box filled with Antifreeze

$\rho_{comb} = 1110\ kg/m^3$, C = 2370. J/kgK

The simulation results are summarized in Figure 5.2A-C. It is clear that the larger heat capacitance of the antifreeze filled box yields a prolonged decay of the dimensionless parameter. The slower heat transfer rate of the antifreeze versus the air filled box in Figure 5.2A correlates with the experimental responses in Figure 4.3 and 4.4.

The correlation for high and low emissivity in the air filled case (.9 and .1, respectively) is depicted in Figure 5.2B. The curve corresponding to an emissivity coefficient of .9 shows a considerable difference in response. The medium with higher emissivity (.9) exhibits a considerably faster response, denoting more heat transfer from the surface.

The modeling also supports the significance of emmisivity. The percentage of the total heat flux due to the radiative term is shown in Figure 5.2C. Although the radiative term is not dominant, it is very significant, especially in free convection.

The above modeling results are derived from a lumped parameter model and are only intended for qualitative analysis of the heat transfer process and verification of experimental results. A higher-order model would have to be developed in order to achieve quantitative results. The experimental responses strongly suggest an acute sensitivity of energy transfer to surface properties and much less sensitivity to specific film gauge or core properties.

Further development of this first-order model is not warranted since the Insulated Box experiments only show the extreme difference between metallic and nonmetallic films. In order to

further investigate effects of the films' radiative properties, such as emissitivity, reflectiveness or absorption, more elaborate experimental work would have to be completed.

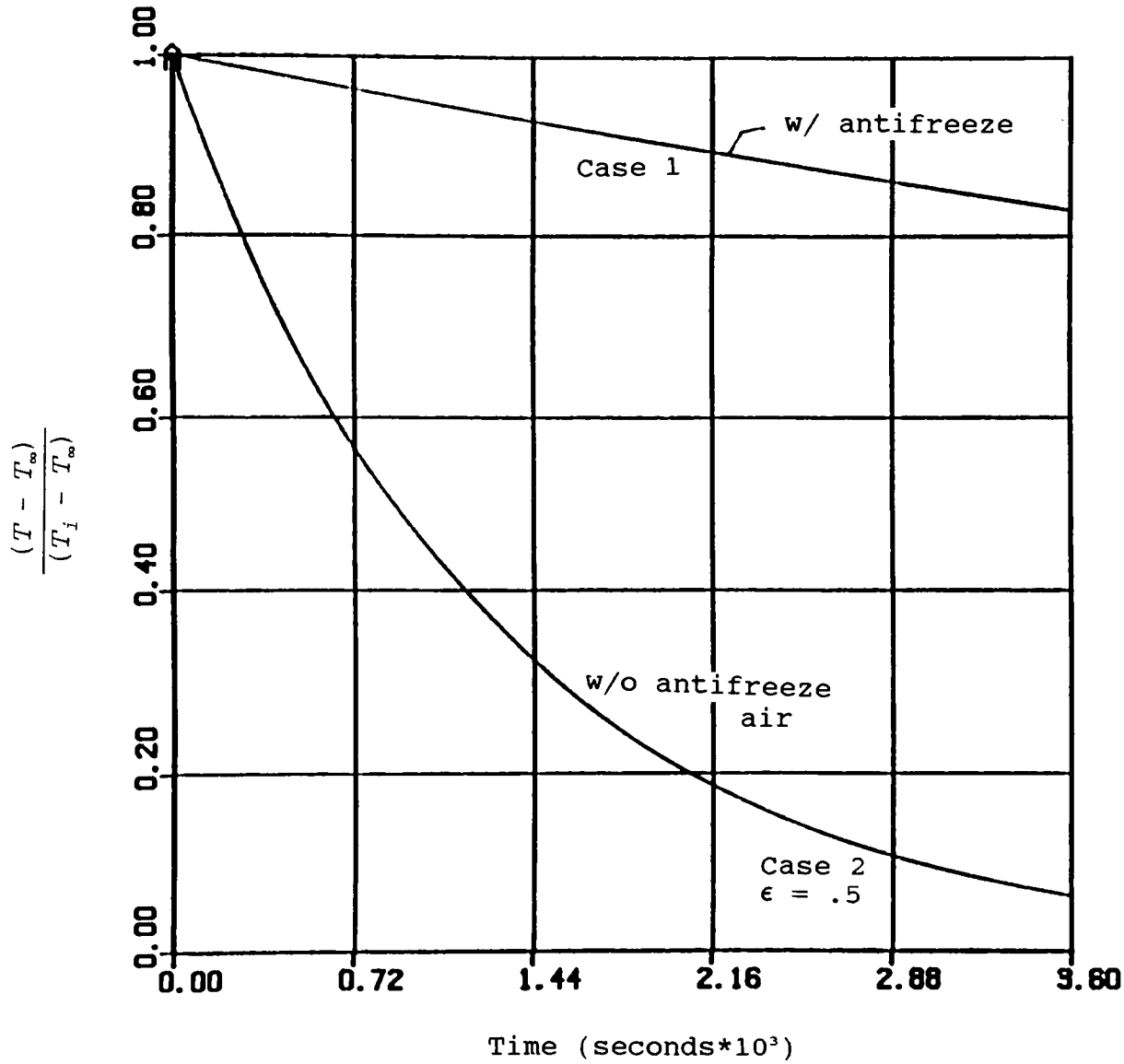

Figure 5.2A
Theoretical freeze cycle with and without antifreeze.

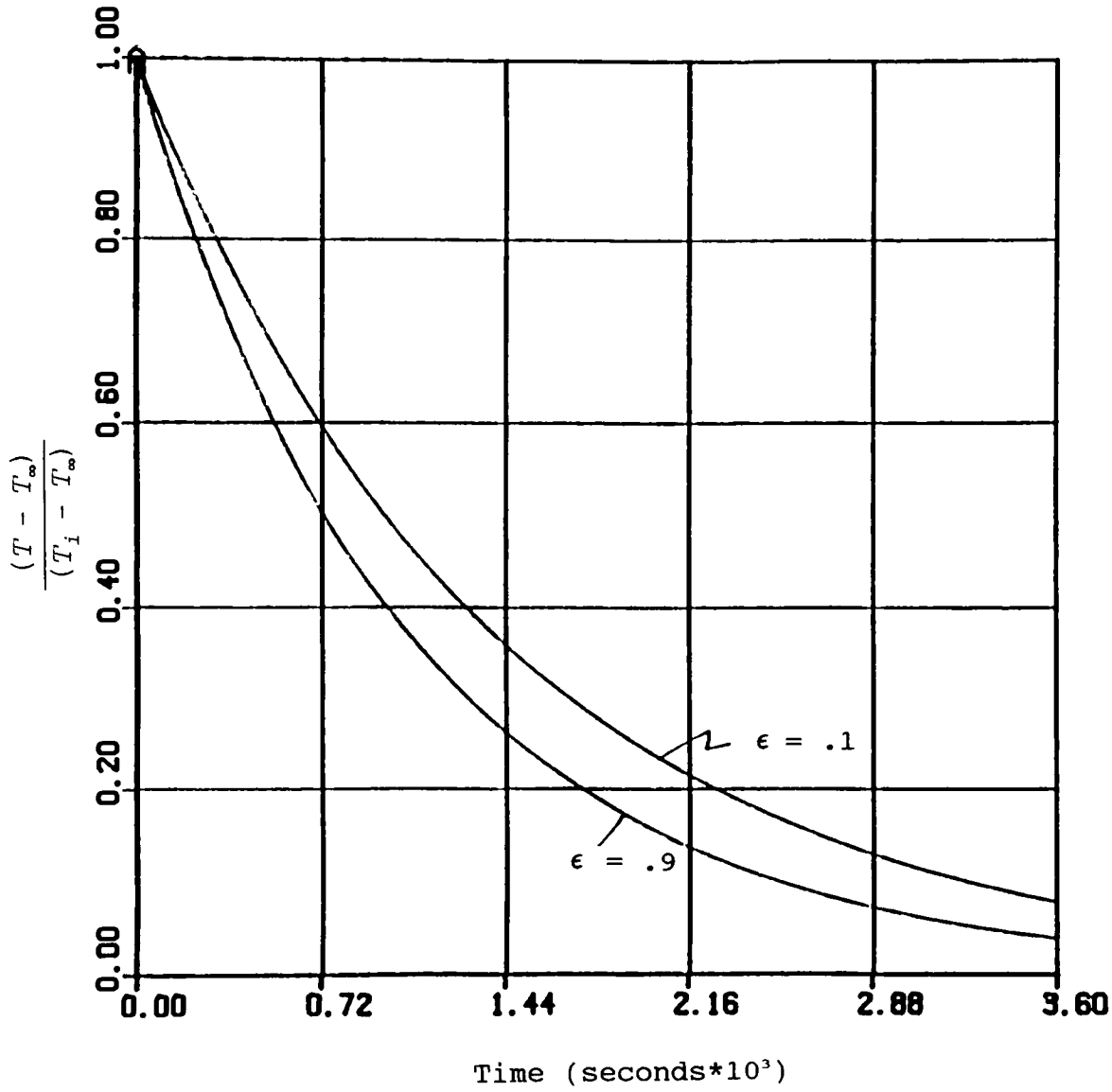

Figure 5.2B
Theoretical freeze cycle with effect of film emissitivity.

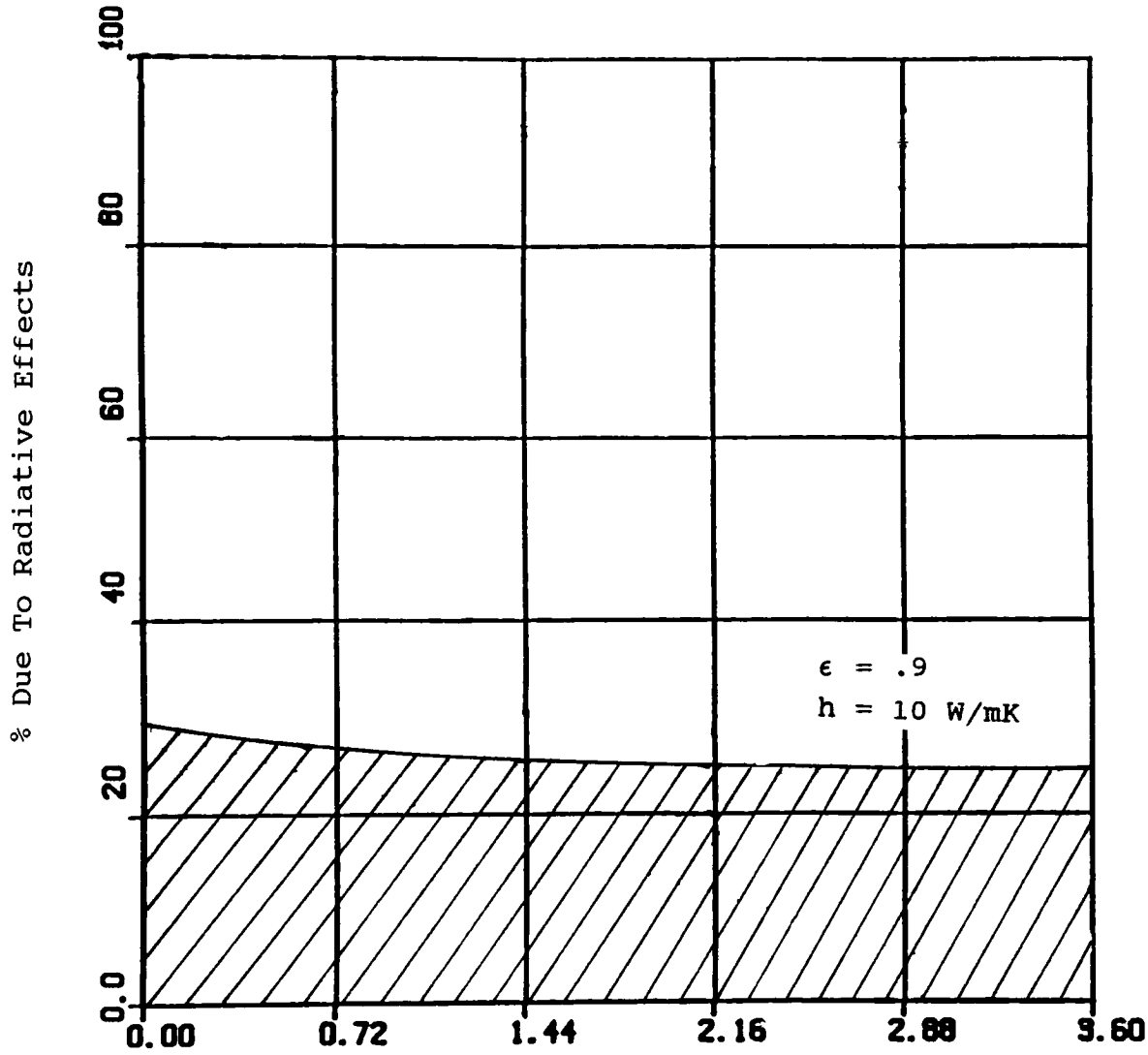

Figure 5.2C
Percent of Heat Flux due to Radiative Effects

5.2 FINITE ELEMENT MODELING THEORY

Finite element methods are based on the local application of variational principles. In a variational framework, a generalized solution to an operator equation is found by minimizing a giving functional. The advantage afforded by a variational formulation is that differentiability properties of solutions are less restrictive and thereby allow for approximate solutions which are only piecewise smooth.

The term "variational formulation" is used contextually to mean the weak formulation, in which weak refers to the fact that a function satisfies a boundary value problem in a certain averaged sense. The differential equation is recast in an equivalent integral form by trading differentiation between a test function and the dependant variable. When the differential operator is symmetric, the weak formulation can be further posed as a minimization problem for a given functional, I(u). From the calculus of variations, the minimizing function is the true solution of the differential equation. For an approximate solution to a variational problem, the primary variable is approximated by a linear combination of appropriately chosen functions:

$$u = \sum_{j=1}^{N} c_j \Phi_j$$

The parameters c_j are determined such that the function u minimizes the functional I(u), ie. u satisfies the weak formulation [5].

In addition to satisfying a governing equation, the solution to a boundary value problem must admit specified values on the boundary of the domain. On the other hand, if the solution or its derivatives are specified initially (ie. at a set time t_o), then it is referred to as an initial-value problem. The equations governing the heat flow in the films represent an initial/boundary value problem. That is, a combination of the above.

In order to appreciate the fundamental principles of the finite element method, one must understand the concepts of functionals and variational operators. Consider the integral expression

$$I(u) = \int_b^a F(x, u, u')\, dx \tag{5.2}$$

where the integrand F(x,u,u′) is a given function of the three arguments x, u, and du/dx. The value of the integral depends primarily upon u, hence I(u) is appropriate. The integral in Eq. (5.2) represents a scalar for any given function u(x). I(u) is called a functional, since it assigns a value defined by integrals whose arguments themselves are functions. Mathematically, a functional is an operator mapping u into a scalar I(u).

A functional l(u) is said to be linear in u if and only if the relation

$$l(\alpha u + \beta v) = \alpha l(u) + \beta l(v)$$

holds for all scalars α, β and functions u and v. A functional of

two arguments, B(u,v), is said to be bilinear, if it is linear in each of its arguments u and v [4].

The integrand, F = F(x,u,u′), depends on the independent variable x and dependent variables u and u′. An infinitesimal change in u is called a variation in u and is denoted by δu. The operator δ will be referred to as the variational operator. The variation, δu of a function u, represents an admissible infinitesimal change in the function u(x). If u is specified on some portion of the boundary, its variation there must be zero, since the specified value cannot be varied. The homogeneous form of the boundary conditions on u must be satisfied by any variation of the function u. The variation δu is arbitrary elsewhere on the boundary.

Boundary conditions play an important role in the derivation of the approximation function. The variational formulation facilitates classification of boundary conditions into essential and natural boundary conditions. For further details, see Reddy [5] Section 2.2.

In the following, the three basic steps in the variational formulation of boundary value problems are outlined. Consider the following differential equation in two dimensions, defined on some domain Ω. It is hypothesized that $F(x,u,u_x,u_y)$ is differentiable, so that

$$\frac{\partial F}{\partial u} - \frac{\partial}{\partial x}\left(\frac{\partial F}{\partial u_x}\right) - \frac{\partial}{\partial y}\left(\frac{\partial F}{\partial u_y}\right) = 0 \quad \textit{within} \quad \Omega \qquad (5.3)$$

along with given boundary conditions.

$$\frac{\partial F}{\partial u_x} n_x + \frac{\partial F}{\partial u_y} n_y = \hat{q} \quad on \quad \Gamma_1, \quad u = u' \quad on \quad \Gamma_2 \qquad (5.3)$$

That is, flux is specified on part of the boundary denoted Γ_1 and the value of the function is specified on the remaining portion Γ_2.

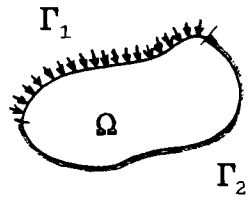

The first step is to multiply Eq. (5.3) by a test function, v, and integrate the product over the domain Ω. The test function can be thought of as a variation in u (δu), which satisfies the homogeneous form of the boundary conditions on Γ_2. V may otherwise be an arbitrary continuous function.

Since Eq. (5.3) is satisfied pointwise, one can integrate both sides over the domain to arrive at the weaker form of Eq. (5.3),

$$0 = \int_\Omega v \left[\frac{\partial F}{\partial u} - \frac{\partial}{\partial x} \left(\frac{\partial F}{\partial u_x} \right) - \frac{\partial}{\partial y} \left(\frac{\partial F}{u_y} \right) \right] dxdy \qquad (5.4)$$

Note that the integral form still contains the same order of differentiation.

The second step involves the transfer of the differentiation from the dependent variable u to the test function v. It is

desirable to transfer the partial derivatives with respect to x and y (u_x & u_y) to v so, that only first-order differentiation is required of both u and v. This results in an equalization of smoothness for both u and v, and thus is a weaker continuity requirement on the solution u to the variational problem. In the process of transferring the differentiation, ie. integration by parts, we obtain the natural boundary conditions. Eq. (5.4) is now expressed as

$$0 = \int_{\Omega} [v\frac{\partial F}{\partial u} + \frac{\partial v}{\partial x}\frac{\partial F}{\partial u_x} + \frac{\partial v}{\partial y}\frac{\partial F}{\partial u_y}]\, dxdy - \oint_{\Gamma} v(\frac{\partial F}{\partial u_x}n_x + \frac{\partial F}{\partial u_y})\, ds \qquad (5.5)$$

The coefficients of v in the second integral represent the natural boundary conditions.

The third step in the formulation consists of simplifying the boundary terms in Eq. (5.5) by applying the specified natural boundary conditions in the problem statement. This is accomplished by splitting the two boundary integrals over the subsets Γ_1 and Γ_2.

$$0 = \int_{\Omega} [v\frac{\partial F}{\partial u} + \frac{\partial v}{\partial x}\frac{\partial F}{\partial u_x} + \frac{\partial v}{\partial y}\frac{\partial F}{\partial u_y}]\, dxdy - \int_{\Gamma_2} v(\frac{\partial F}{\partial u_x}n_x + \frac{\partial F}{\partial u_y}n_y)\, ds - \int_{\Gamma_1} v\hat{q}ds \qquad (5.6)$$

The first boundary integral vanishes, since v is specified ($\delta u=0$) on Γ_2. The variational formulation thus results in a reduction of order as well as an automatic imposition of the natural boundary conditions.

The weak form, Eq. (5.4), finally reduces to

$$0 = \int_{\Omega} [v\frac{\partial F}{\partial u} + \frac{\partial v}{\partial x}\frac{\partial F}{\partial u_x} + \frac{\partial v}{\partial y}\frac{\partial F}{\partial u_y}]\, dxdy - \int_{\Gamma_1} v\hat{q}ds \qquad (5.7)$$

The function u is said to be a weak solution of Eq. (5.3), if u satisfies Eq. (5.7) for all appropriate test functions v. Eq. (5.7) can be more compactly stated in terms of a bilinear functional B(u,v) and a linear functional l(v) as

$$B(v,u) = l(v)$$

for all admissible test functions v.

In Eq. (5.7),

$$B(v,u) = \int_{\Omega} [v\frac{\partial F}{\partial u} + \frac{\partial v}{\partial x}\frac{\partial F}{\partial u_x} + \frac{\partial v}{\partial y}\frac{\partial F}{\partial u_y}]\, dxdy$$

$$and \qquad (5.8)$$

$$l(v) = -\int_{\Omega} vdxdy + \int_{\Gamma_1} v\hat{q}ds$$

If the bilinear form B(v,u) is symmetric, ie B(v,u)=B(u,v), then the quadratic functional associated with the variational formulation is deduced as

$$I(u) = \tfrac{1}{2}B(u,u) - l(u). \qquad (5.9)$$

Satisfying Eq. (5.9) is equivalent to minimizing I(u). When the functional I(u) is in this form, approximate methods, such as the Rayleigh-Ritz Method [5], may be used to minimize the functional.

An approximate method for solution of the weak form, Eq. (5.7), is known as the Galerkin Method. The solution u takes on the

form

$$u_N = \sum_{J=1}^{N} c_j \phi_j$$

in which Φ_j, the approximating basis functions, must satisfy the following conditions:

1) They must be well defined and nonzero as well as sufficiently differentiable as required by the bilinear form $B(\cdot,\cdot)$
2) Any set $\{\Phi_i\}(i=1,N)$ must be linearly independent
3) $\{\Phi_i\}(i=1,\infty)$ must be complete.

These conditions guarantee convergence to the solution. For further discussion of the above conditions, the reader should consult Reddy [5] Section 2.3. When defining the test function, knowledge of the anticipated solution as well as satisfaction of any essential or natural boundary conditions should be taken into account.

The Galerkin approximation is expressed as

$$u_N = \sum_{J=1}^{N} c_j \phi_j(x) \tag{5.10}$$

and the test function is correspondingly written as

$$v = \sum_{i=1}^{m} b_i \phi_i \tag{5.11}$$

If the approximate solution Eq. (5.10) and the test function Eq. (5.11) is introduced into Eq. (5.8), the problem is then reduced to find c_j, such that

$$B\left(u_N=\sum_{J=1}^{N} c_j\phi_j(x)\ ,\ v_m=\sum_{i=1}^{M} b_i\phi_i(x)\right) = F\left(\sum_{j=1}^{M} b_j\phi_j\right) \qquad (5.12)$$

for arbitrary constants b_j.

If $B(\cdot,\cdot)$ and $F(\cdot)$ are linear, an equivalent formulation is

$$\sum_{j=1}^{N} c_j B(\Phi_j, \Phi_i) = F(\Phi_i) \qquad for\ \ i = 1,\ldots,N \qquad (5.13)$$

Eq. (5.13) represents a linear system of equations in the unknown coefficients c_j.

Alternatively, one can set

$$\int_\Omega (Au-f)\, v\phi_j(x)\, d\Omega \ + \ B.C.'s\ \ Terms \ = \ 0$$

where A is a linear operator defining

$$Au = f$$

on the domain Ω.

5.3 THERMAL ANALYZER

5.3.1 Galerkin Approximation

The thermal analyzer apparatus (see Figure 3.2) can be modeled by assuming one-dimensional heat flow, with all heat energy being transferred through the film from the bottom aluminum block to the upper block. The film is very thin in comparison to the dimensions of the aluminum blocks. Further, with the edges being insulated, the only heat transfer is in the direction perpendicular to the block surfaces with minimal edge effects. The response is rapid enough so that any convection taking place on the edge is negligible. Figure 5.3 below depicts the model schematically with the associated boundary conditions at the heat source and insulation barrier.

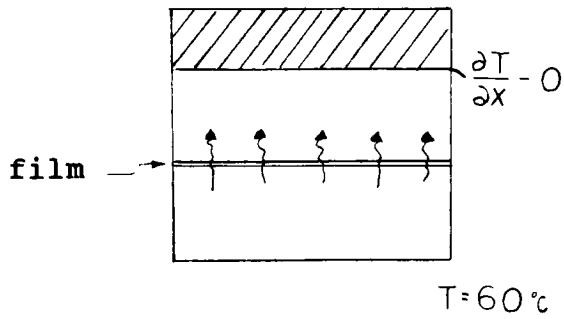

Figure 5.3

Mathematically, the film can be represented as a discontinuity in the material properties of the two conducting aluminum plates. The conducting composite medium is modeled as two domains divided by a thin conducting film layer.

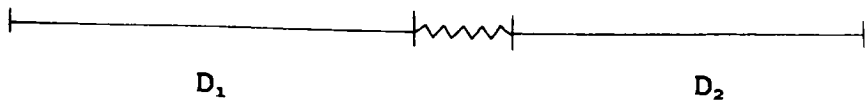

Conduction through any medium within the subdomains is governed by the standard transient heat conduction equation,

$$\alpha \frac{\partial^2 T}{\partial x^2} = \frac{\partial T}{\partial t} \tag{5.13}$$

The domains D_1 and D_2 represent the conducting aluminum blocks. T(x,t) is the instantaneous temperature distribution within the domains and

$$\alpha = k/(\rho c)$$

is the thermal diffusivity of aluminum. Separating the two domains is an extremely thin film layer. The temperature distributions in the aluminum domains will be approximated using appropriate Galerkin shape functions, whereas the film temperature profile will be assumed to be linear, due to the very small thickness of the film. The instantaneous temperature profile in the apparatus model is depicted in Figure 5.4.

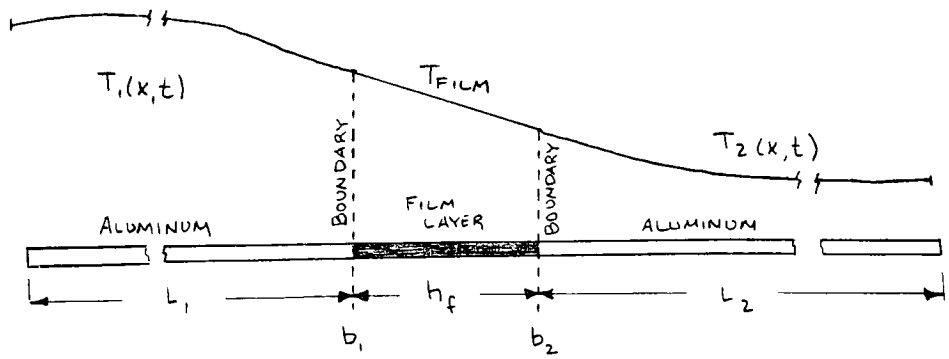

Figure 5.4
Temperature distribution in the domains.

The overall temperature is comprised of three temperature distributions, coupled at the contacting boundaries by flux and temperature continuity. Specifically, the conditions

$$T_{al}|_{b1} = T_f|_{b1}$$

$$T_f|_{b2} = T_{al}|_{b2}$$

$$k_{al}\frac{\partial T}{\partial X}\Big|_{b1} - k_f\frac{\partial T}{\partial X}\Big|_{b1} \qquad (5.14)$$

$$k_f\frac{\partial T}{\partial X}\Big|_{b2} - k_{al}\frac{\partial T}{\partial X}\Big|_{b2} \qquad (5.15)$$

are imposed at the film boundaries b_1 and b_2. The coefficients k_{al} and k_f in Eqs. (5.14) and (5.15) are the thermal conductivities of the aluminum and film, respectively.

The motivation of this modeling is to simulate the response of the two thermocouples placed in the aluminum blocks close to the film surface. An analytical model, based on a semi-discrete Galerkin approximation, is presented below.

The Galerkin approximation is based on a variational formulation of Eq. (5.12) on the domains D_1 and D_2. Appropriate shape functions Φ_1, Φ_2 and Φ_3 are required to satisfy the known essential boundary conditions. A(t), B(t) and C(t) identify with the time-dependant amplitudes of the shape functions associated with the responses at each thermocouple. In particular, the temperature distributions in the aluminum plates are

hypothesized as

$$T_1(x,t)=A(t)\Phi_1(x) \quad + 60^\circ \tag{5.16}$$

$$T_2(x,t)=B(t)\Phi_2(x) - C(t)\Phi_3(x) + 20^\circ \tag{5.17}$$

The shape functions Φ_1, Φ_2 and Φ_3 must satisfy the boundary conditions

$$\Phi_1(0,t) = 0 \quad \& \quad B\Phi'_2(L_2,t) - C\Phi'_3(L_2,t)= 0$$

Transforming the governing differential equation (5.12) into the variational form, appropriate terms are then integrated by parts. By implementing the boundary conditions, the equation becomes simplified. For each domain:

$$\int_0^L [\alpha \frac{\partial T_i}{\partial x}\cdot\frac{\partial V}{\partial x}+\frac{\partial T_i}{\partial t}\cdot V]\,dx- \quad \alpha\frac{\partial T_i}{\partial x}\cdot V\Big|_0^L \tag{5.18}$$

where T_i represents the temperature distribution in domain D_i and $V(x)$ is the test function associated with the Galerkin method, specifically Φ_i. Substitution of the temperature shape functions, Eqs. (5.16) and (5.17), into the variational form Eq. (5.18), results in two ordinary differential equations for the time-varying amplitudes:

$$K_{11}A + K_{12}\dot{A} = P^1{}_2\Phi_1(L_1) \tag{5.19}$$

$$\begin{vmatrix} K_{22} & K_{23} \\ K_{32} & K_{33} \end{vmatrix} \begin{vmatrix} B \\ C \end{vmatrix} + \begin{vmatrix} R_{22} & R_{23} \\ R_{32} & R_{33} \end{vmatrix} \begin{vmatrix} \dot{B} \\ \dot{C} \end{vmatrix} - P_1^2 \begin{vmatrix} \Phi_2(0) \\ \Phi_3(0) \end{vmatrix} \tag{5.20}$$

These two differential equations are coupled by continuity of temperature and flux at the contacting boundaries. That is,

$$P_2^1 = -\alpha \left.\frac{\partial T_1}{\partial x}\right|_{x=L_1}$$

$$-\frac{\alpha}{k_a} \cdot k_a \left.\frac{\partial T_1}{\partial x}\right|_{x=L_1} = -\frac{\alpha}{k_a} \cdot k_f \quad \frac{B\phi_2(0) - A\phi_1(l_1) - 40}{h_f}$$

$$-\frac{\alpha}{k_a} \cdot k_a \left.\frac{\partial T_2}{\partial x}\right|_{x=0}$$

$$= -P_1^2$$

Eqs. (5.19) and (5.20) can thus be expressed as a system of equations

$$K_{11}A + K_{12}\dot{A} = \frac{\alpha}{h_f} \cdot \frac{k_f}{k_a} [B\phi_2(0) - A\phi_1(L_1) - 40] \cdot \phi_1(L_1)$$

$$\begin{vmatrix} K_{11} & K_{12} \\ K_{21} & K_{22} \end{vmatrix} \begin{vmatrix} B \\ C \end{vmatrix} + \begin{vmatrix} R_{11} & R_{12} \\ R_{21} & R_{22} \end{vmatrix} \begin{vmatrix} \dot{B} \\ \dot{C} \end{vmatrix} = -\frac{\alpha}{h_f} \cdot \frac{k_f}{k_a} [B\phi_2(0) - A\phi_1(L_1) - 40] \begin{vmatrix} \phi_2(0) \\ \phi_3(0) \end{vmatrix}$$

The initial temperatures of the top and bottom blocks are 20°C and 60°C, respectively. A linear transformation for the simulated temperature profiles is utilized to allow for the initial values A(0) = B(0) = C(0)= 0. The equations are then solved for A(t), B(t), and C(t) which results in the temperature profiles

$$T_1(x,t) = A(t)\Phi_1(x) + 60^\circ$$

$$T_2(x,t) = B(t)\Phi_2(x) - C(t)\Phi_3(x) + 20^\circ$$

The locations of the thermocouples are specified by $x=p_i$ (i=1,2). Thus the corresponding thermocouple responses are given by:

$$T_1(p_1,t) = A(t)\Phi_1(p_1)+60^{\circ}$$

$$T_2(p_2,t) = B(t)\Phi_2(p_2) - C(t)\Phi_3(p_2) +20^{\circ}$$

The shape functions were chosen as $\Phi_1 = \sin(x)$, $\Phi_2 = 1$ and $\Phi_3 = \sin(\pi x/2*L_2)$, since these satisfy the known boundary conditions.

The weak formulation on each domain is summarized below.

$$D_i: \int (\alpha \frac{\partial T^2}{\partial x^2} + \frac{\partial T}{\partial t})\, v dx = 0 \quad \textit{Weak formulation}$$

$$\int (\alpha \frac{\partial T}{\partial x}\frac{\partial v}{\partial x} + \frac{\partial T}{\partial t} v)\, dx = [\alpha \frac{\partial T}{\partial x} v]$$

On D_1 :

$$D_1: \int_0^{L_1} (\alpha \frac{\partial T}{\partial x}\frac{\partial v}{\partial x} + \frac{\partial T}{\partial t} \cdot v)\, dx = P_2^1 V(L_1) \qquad (5.21)$$

On D_2 :

$$D_2: \int_0^{L_2} (\alpha \frac{\partial T}{\partial x}\frac{\partial v}{\partial x} + \frac{\partial T}{\partial t} \cdot v)\, dx = P_1^2 V(0) \qquad (5.22)$$

The respective Galerkin approximations were chosen as

$$T = A(t)\Phi_1 + 60^{\circ}, \text{ (on } D_1)$$

$$T = B(t)\Phi_2 - C(t)\Phi_3 + 20^{\circ}, \text{ (on } D_2)$$

where: $\Phi_1 = \sin(x)$ and

$\Phi_2 = 1$

$\Phi_3 = \sin(\pi x/2*L_2)$.

The shape functions Φ_i are substituted for v in Eqs. (5.21) and (5.22). Since $\frac{\partial T_1}{\partial x} = A\phi_1'$ and $\frac{\partial T_2}{\partial x} = B\phi_2' - C\phi_3'$, it follows that

$$\int_0^{L_1} (\alpha_1 A \phi_1' \phi_1' + \dot{A}\phi_1\phi_1)\, dx = P_2^1 \phi_1(L_1) \tag{5.23}$$

$$\int_0^{L_2} (\alpha_2 (B\phi_2' - C\phi_3')\, \phi'_i + (\dot{B}\phi_2 + \dot{C}\phi_3)\, \phi_i\, dx = P_1^2 \phi_i(0)) \quad for\ i=1,2 \tag{5.24}$$

Since the temperature distribution in the film is assumed to be linear, continuity of flux at each contacting surface requires:

$$k_{al} \frac{\partial T_1}{\partial x}\bigg|_{L_1} = k_f \frac{\Delta T}{h} = k_{al} \frac{\partial T_2}{\partial x}\bigg|_{L_2}$$

$$Now: \quad k_a \frac{\partial T}{\partial x}\bigg|_{x=L_1} = k_f = k_{al} \frac{(B\phi_2(0) - A(\phi_1(l_1)) - 40)}{h}$$

$$So, \quad P_2^1 = \alpha \frac{\partial T}{\partial x}\bigg|_{x=L_1} = \frac{\alpha K_f \cdot \Delta T}{K_a \cdot h} \tag{5.25}$$

Integrating Eqs. (5.23) and (5.24) :

On D_1:

$$A\alpha \int_0^{L_1} \cos^2(x)\, dx + \dot{A} \int_0^{L_1} \sin^2(x)\, dx = P_2^1 \sin(L_1)$$

$$\therefore \quad A\alpha \left[\frac{1}{2}L_1 + \frac{1}{4}\sin(2L_1)\right] + \dot{A}\left[\frac{1}{2}L_1 - \frac{1}{4}\sin(2L_1)\right] =$$

$$\frac{\alpha k_f}{k_a h_f} [b - A\sin(L_1) - 40] \sin(L_1) \tag{5.26A}$$

On D_2:

Integrating with respect to Φ_2:

$$\int_0^{L_2} (\dot{B} - \dot{C}\sin(\frac{\pi x}{2L_2})) \cdot 1 dx = P_1^2 \cdot 1$$

$$\therefore \quad \dot{B}L_2 - \dot{C}\frac{2L_2}{\pi} = -\frac{\alpha K_f}{K_{al} h_f} [B - A\sin(L_1) - 40]$$

Integrating with respect to Φ_3:

$$-\alpha (\frac{\pi}{2L_2})^2 C \int_0^{L_2} \cos^2(\frac{\pi x}{2L_2}) dx + \int_0^{L_2} (\dot{B} - \dot{C}\sin(\frac{\pi x}{2L_2})) \cdot \sin(\frac{\pi x}{2L_2}) dx = P_1^2 \cdot 0$$

$$\therefore \quad -\alpha \frac{\pi^2}{8L_2} C + \frac{2L_2}{\pi} \dot{B} - \frac{L_2}{2} \cdot = 0$$

Rewriting the two equations representing D_2:

$$-\frac{\pi^2 \alpha}{8L_2} C + (\frac{8L_2 - \pi^2 L_2}{2\pi^2}) \dot{C} = \frac{2}{\pi} P_2^1 \qquad (5.26B)$$

$$\frac{2L_2}{\pi} \dot{B} - \frac{\pi^2 \alpha}{(8-\pi^2) L_2} C = \frac{2\pi}{8-\pi^2} P_2^1 \qquad (5.26C)$$

Eqs. (5.26A-C) represent the final form of the equations governing the amplitude variation and are simultaneously solved for $\dot{A}$ and $\dot{B}$. In the standard form, the coupled first-order system of differential equations is expressed as

$$\dot{A} = \frac{[(\frac{\alpha k_f}{k_a h_f})[(B-A\sin(L_1)-40.)\cdot\sin(L_1)]-A\alpha(\frac{1}{2}L_1+\frac{1}{4}\sin(2L_1)]}{[\frac{1}{2}L_1-\frac{1}{4}\sin(2L_2)]} \quad (5.27A)$$

$$\dot{B} = \frac{\pi^2}{(8-\pi^2)2L_2^2}(\alpha C+L_2\frac{\alpha k_f}{k_a h_f}[(B-A\sin(L_1)-40.]) \quad (5.27B)$$

$$\dot{C} = \frac{(\frac{\pi^4\alpha}{4L_2}C+4\pi\frac{\alpha K_f}{K_a h_f}[(B-Asin(L_1)-40])}{8L_2-\pi^2 L_2} \quad (5.27C)$$

The input parameters are listed below.

T_{tot} = 45 or 60 seconds	Response time
L_1 = .0013 m	Location of bottom thermocouple
L_2 = .009525 m	Thickness of top aluminum block
H_f = 2.54E-5 - 2.54E-4m	Thickness of thin film
D_1 = .00127 m	Depth of thermocouple 2
α = 68.2E-06 m2/s	Thermal diffusivity of Al
k_a = 168. W/mK	Conductivity of Al
k_f = .01 - 1.0 W/mk	Conductivity of thin film

The temperature response at each thermocouple location is computed as

$$T_{tc1} = A*\sin(X_{tc1}) + 60^\circ \quad (5.28)$$

$$T_{tc2} = B*1 - C*\sin(\pi X_{tc2}/2L_2)) + 20^\circ \quad (5.29)$$

5.3.2 Determination of Apparent Conductivities

Eqs. (5.27 A-C) are solved using a dynamic simulation software package known as ACSL (Advanced Continuous Simulation Language). The response at each thermocouple is specified as the final output in Eqs. (5.28) and (5.29). The apparent thermal conductivity of the film, k_{app}, and the thickness Δx of the film layer are considered as input parameters. Thus, Eqs. (5.27 A-C) were repeatedly solved for various values of the input parameters with appropriate thermocouple responses as output.

To deduce the apparent conductivity, k_{app}, of a given gage of film, the simulated responses and the experimental responses are overlaid. If these responses qualitatively agree, a trial value of k_{app} is substantiated. Specifically, by testing of all the films experimentally with the thermal analyzer, each k_{app} can be estimated by fitting the experimental response to the simulated responses corresponding to each given thickness. Noting Figure 5.5, simulated responses (solid lines) are plotted for a given thickness of 1.40 mils and various assumed thermal conductivities. An experimental response from the Thermal Analyzer of 1.40 mil uncoated OPPalyte is overlaid and one can readily estimate the film conductivity. From Figure 5.5, the thermal conductivity appears to be

$$k_{app} = .022 \text{ W/mK}$$

Table 4.1 lists all of the k_{app} values for each of the films tested.

One should note, however, that these comparisons are subjected to any inherent errors in the thermal analyzer experiments. Consequently, the values of conductivity are apparent and can be

only established on a relative and comparative basis with other films tested under the same conditions.

Published values of very thin materials vary greatly due to the variety of experimental techniques. In the Thermal Analyzer, surface contact between the film and aluminum blocks is one of the correction factors that must be incorporated to find an absolute conductivity. Since this contact resistance also exists in real life applications as well, no correction is made for simulations.

To obtain absolute conductivities one would have to establish an errorless thermal analyzer and transducer, establish a thickness-to-conductivity relation for the given samples, or correlate a surface contact factor derived from a no-film test to an apparent conductivity.

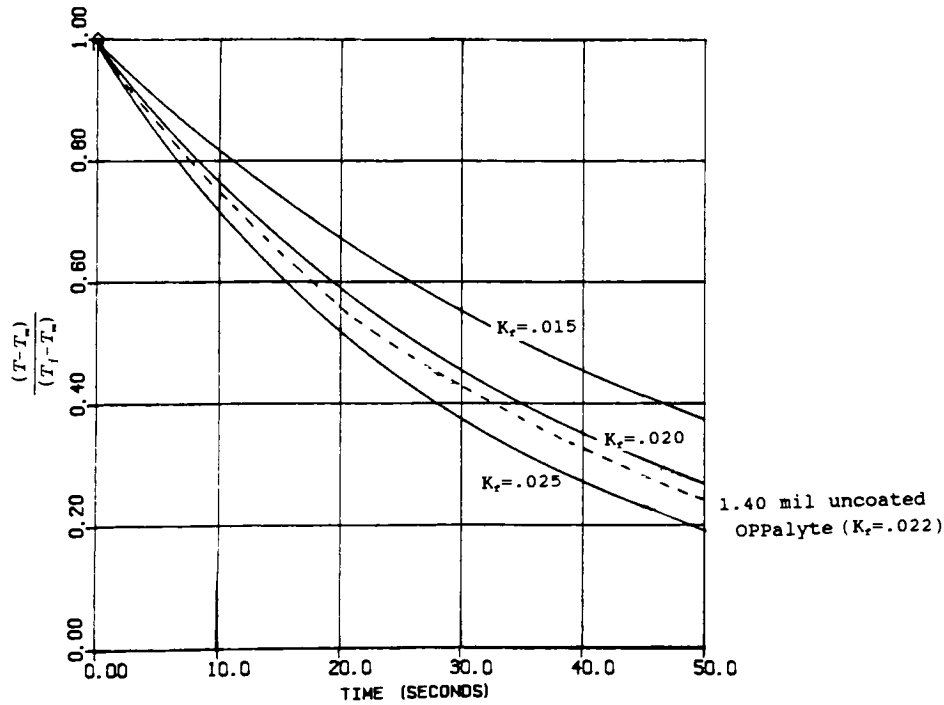

Figure 5.5
System response for selected values of k_f.

Table 5.1
Material List with apparent k

MATERIAL	GAGE (mils)	Kapp W/mK
1. 1.10 mil uncoated OPPalyte(TM)	1.13	.025
2. 1.50 mil uncoated OPPalyte	1.55	.026
3. 1.40 mil uncoated OPPalyte	1.27	.022
4. 2.00 mil uncoated OPPalyte	1.61	.0235
5. 2.50 mil uncoated OPPalyte	2.34	.0225
6. 1.60 mil coated OPPalyte	1.59	.0275
7. 1.50 mil coated OPPalyte	1.34	.024
8. 1.00 mil/1.00 mil uncoated OPPalyte	1.89	.032
9. 1.10 mil/1.10 mil uncoated Oppalyte	2.36	.035
10. metallized/1.50 mil uncoated OPPalyte	1.32	.025
11. 1.40 mil coextruded oriented polypropylene	1.42	.040
12. 1.00 mil coextruded oriented polypropylene	.98	.032
13. .80 mil coextruded oriented polypropylene	.79	.037
14. Poly coated paper	3.50	.028
15. Foil/paper	2.65	.070
16. waxed paper	1.35	.050*
17. aluminum foil	.72	.051
18. chipboard	16.75	.058
19. 2.50 mil uncoated OPPalyte/chipboard		.058
20. white pigmented polyethylene	1.50	.075
21. polyester	.59	.032
22. high opacity sealable white opaque	1.77	.020
23. Hercules white opaque OPP	1.61	.032
24. 1.10 mil coated OPPaLYTE/.75 mil cellephane	1.82	.031
25. 1.00 mil coex OPP/1.00 mil coex OPP	2.10	.060
26. 1.40 mil Metallyte(TM)	1.45	.035
27. Hercules metallized white opaque OPP	1.61	.042
28. 2.75 mil white low density polyethylene	2.77	
29. 2.35 mil white low density polyethylene	2.40	.075
30a.7.5 polystyrene foam	5.95	.029
30b.11.0 mil polystrene foam	11.0(?)	.0225
31. Metalized polyester/white polyester	1.97	.070
32. Poly coated paper (Ice cream wraps)	2.01	.050

(TM) = Trademark
OPPalyte = Trademark name for all Mobil white opaque films
Metallyte = Trademark name for all Mobil metallized films
OPP = oriented polypropylene

* Note : Waxpaper when tested seemed to "melt" under the thermal analyzer temperature and any conclusions about waxpaper could be faulty.

5.4 Freezer Environment

Response Characteristics Associated with a Freezer Environment

Once the apparent heat transfer parameters of the films are quantitatively established, one can use this information for modeling and simulation in environments associated with various thin film applications.

One specific aspect that is most crucial to the packaging of frozen dairy products within a typical freezer environment is the automatic defrost cycle. In the defrost cycle, temperatures rise above 0° C, where most freezer commodities such as ice cream or vegetables can momentarily thaw. This defrost cycle can be potentially detrimental to the package contents. If partially unfrozen, then refrozen, the package contents will undergo freezer burn and may be damaged. Frozen liquid items may leak and eventually refreeze into undesirable shapes.

Manufacturers are seeking the development of films that will better protect perishable items from permanent damage, such as freezer burn. The objective of modeling the response of a product in a freezer environment is to ascertain whether a relative difference in film properties will actually cause a substantial improvement in the protection of a product.

The developed model simulates the response of a perishable item wrapped in various film enclosures. The response profiles were determined for a variety of film parameters, such as conductivity

and thickness, as well as for different freezer environments. The profiles can be compared to see if any change in the conductivity results in a substantial change of temperature response within a package. The expense in the manufacturing of a new composite film would have to be justified by a definite improvement of protective property.

The food commodity is first discretized for finite element modeling. The product domain is bounded by thin layers of film, generating contact boundary conditions. The different modes of heat transfer, namely, conduction, convection and radiation are considered individually to ascertain the relative influence upon the response of the model. The possible boundary conditions at the film surface can be numerous, therefore, only a few conditions are examined in detail. The primary cases are delineated as

1) Pure conduction: The film is in contact with another solid (ie. food commodity package).
2) Pure convection: The film is in contact with a fluid (ie. air) that has an associated convection coefficient, h (W/m^2K).
3) Convection and radiation: The film exterior, assumed to be metallized, is exposed to the ambient freezer environment.

In order to realistically model the thermal response, several variations in ambient temperature fluctuations were investigated. These consist of

A) Harmonic : A ramp, constant and fall of temperature to

simulate a defrost cycle.

B) Ramp : A constant rise and leveling of temperature to simulate leaving the frozen commodity exposed to room temperature.

C) Pulse : Subjecting the frozen item to a warmer environment for a short period of time then refreezing.

These freezer environment variations are shown in Figure 5.6.

INPUT # 1 (Rise-constant-fall)

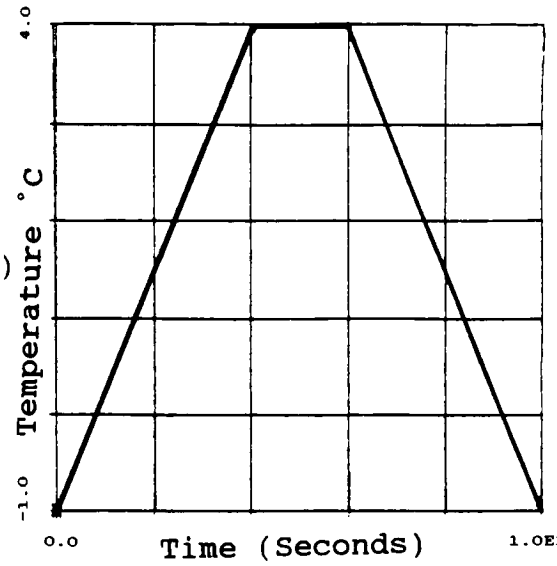

INPUT # 2 (Rise-constant)

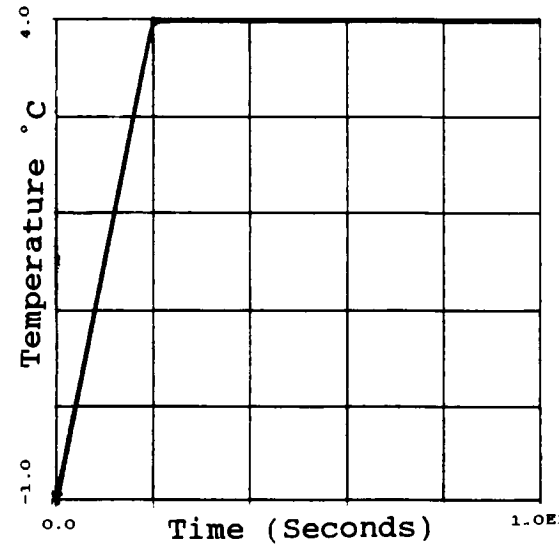

INPUT # 3 (Pulse)

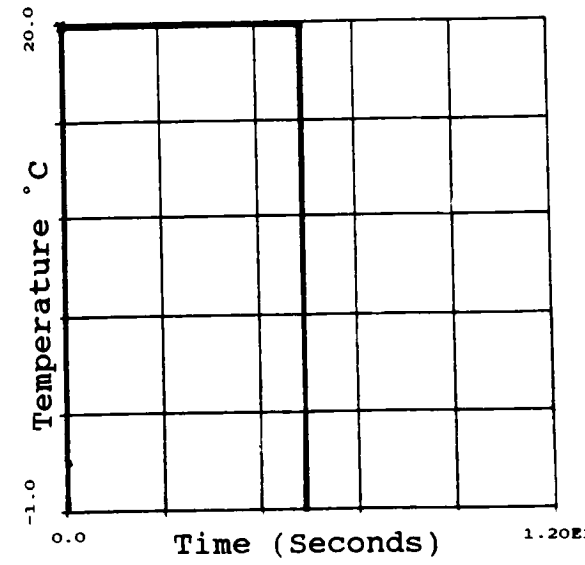

Figure 5.6
Various input temperature profiles.

5.4.2 Dynamic Model Formulation

Finite element modeling was utilized in order to model the packaged product in a typical freezer environment. The modeling will be restricted to one-dimensional transient heat transfer, since the film thickness is extremely small in comparison to the size of the packaged commodity. The dominating heat transfer mechanism is perpendicular to the film surface and edge effects render no significance. Another assumption was that only one side of the food commodity is exposed to freezer conditions and the other side is adjacent to another package or the freezer wall.

The package domain was discretized into 10 elements with an adjacent film boundary. The film is not discretized, since it is extremely thin and the temperature distribution in the film can be assumed to be linear.

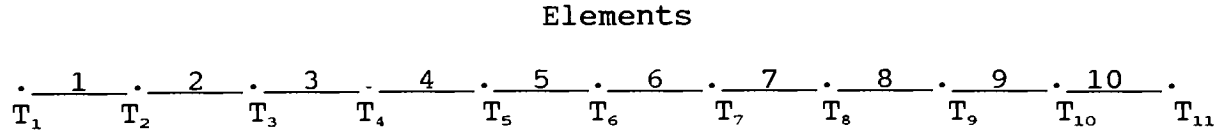

Figure 5.7

The package size was assumed to be 3 inches in thickness with each element measuring .3 inches. In Figure 5.7, T_{11} represents the temperature at the contact surface between the packaged commodity and the film enclosure. The nodal temperatures are time dependent,

governed by the transient heat conduction equation. Once the film boundary conditions are imposed, the model is quantitatively represented as a tenth-order system of ordinary differential equations.

The boundary conditions, described above, couple the individual equations by requirements of flux continuity and temperature continuity at element boundaries. The dynamical system is developed as follows.

The local equation for each individual element is

$$[\ K\ ]^e[\ T\ ] + [\ R\ ]^e[\dot{T}] = [f]^e \qquad (5.30)$$

where K is the stiffness matrix, R is the dissipation matrix and f is the generalized force vector. Expressing the conduction equation

$$\alpha \frac{\partial^2 x}{\partial t^2} = \frac{\partial T}{\partial t} \qquad (5.31)$$

in the weak form over each individual element, the element equations are given by

$$\frac{\alpha^e}{h^e}\begin{vmatrix} 1 & -1 \\ -1 & 1 \end{vmatrix} + \frac{h^e}{6}\begin{vmatrix} 2 & 1 \\ 1 & 2 \end{vmatrix} = \begin{vmatrix} P_1^1 \\ P_2^1 \end{vmatrix} \qquad (5.32)$$

Next, the element matrices are assembled with adjoining

element matrices to produce a global system for the entire discretization.

$$\frac{\alpha}{h}\begin{vmatrix} 1 & -1 & 0 & & & & 0 \\ -1 & 2 & -1 & & & & \\ 0 & -1 & 2 & & & & \\ & & & \ddots & & & \\ & & & & 2 & -1 & 0 \\ & & & & -1 & 2 & -1 \\ 0 & & & & 0 & -1 & 1 \end{vmatrix} + \frac{h}{6}\begin{vmatrix} 2 & 1 & 0 & & & & 0 \\ 1 & 4 & 1 & & & & \\ 0 & 1 & 4 & & & & \\ & & & \ddots & & & \\ & & & & 4 & 1 & 0 \\ & & & & 1 & 4 & 1 \\ 0 & & & & 0 & 1 & 2 \end{vmatrix} = \begin{vmatrix} P_1^1 \\ 0 \\ \\ \\ 0 \\ P_2^{10} \end{vmatrix} \tag{5.33}$$

Eq. (5.33), in its present form, cannot be solved, since at this point there are too many unknowns. The system is made determinate by applying the initial and boundary conditions, after which the modified system can be solved. P_2^{10} contains the film boundary condition at the exterior surface and is determined by the appropriate specifications inherent to exterior interaction through conduction, convection, or radiation & convection.

The T_1 boundary condition contains both $T_1(0)$ and $\dot{T}_1(0)$. In the present case, $\dot{T}_1(0)=0$, by assuming that node 1 of the commodity contacts either another commodity at the same temperature or ice at a fixed temperature. Also, for simplicity, it is also assumed that $T_1(0)=0$. The initial value at T(0) can be changed to accommodate any case by adding appropriately to the right hand side [F].

Eq. (5.32) is put into standard form by premultiplying it with R^{-1}, to obtain

$$[\ R^{-1}\ ][\ K\ ][\ T\ ] + [\ \dot{T}\ ] = [\ R^{-1}\ ][\ F\ ]$$

from which

$$[\ \dot{T}\ ] = -[\ R^{-1}\ ][\ K\ ][\ T\ ] + [\ R^{-1}\ ][\ F\ ] \qquad (5.34)$$

The final form of Eq. (5.34) is shown as a system of differential equations listed a Fortran list file in the Appendix.

5.4.3 Summary of Freezer Simulation Results

A number of cases were investigated, ranging from different freezer environments to different modes of heat transfer. All of the freezer environments were characterized by pulse-like temperature profiles resulting in a dynamic response represented by a thermal wave of energy propagating through the medium. As the thermal wave propagates along the spatial, the amplitude of the temperature is damped due to the internal energy diffusion within the package contents. This thermal wave propagation differs from model to model, depending on the inputed temperature variations and associated boundary conditions (See Figures 5.8 - 5.10). As expected, the nodal temperatures closest to the film boundary are the most sensitive to the input temperature variation.

A change in the primary heat transfer mode on the film surface or the environmental fluctuation resulted in a different frequency and amplitude of the propagating thermal wave. It is interesting to note that a change in thickness or conductivity of the film, given an input response, results only in an amplitude change of the thermal wave and not a frequency change. Since the amplitude is actually the magnitude of temperature, one can comparatively differentiate the relative barrier properties associated with various film thicknesses and thermal conductivities. Since the nodal temperature closest to the film is the most sensitive, the

thermal barrier properties of different films will be analyzed for the temperature response at T_{11}. Recall that node 11 represents the surface of the product which is in contact with the film enclosure.

The comparison will be instituted as a percent difference in the peak values of temperature across the film boundary, T_{11} and ambient temperature T_{inf}. This usually occurs near the end of the simulation run. In particular,

$$\text{insulative sensitivity} = \frac{(T_{11}-T_{inf})*100}{T_{inf}}$$

The various film parameters, namely, conductivity and thickness, are compared as a change in insulative sensitivity. The results of this simulation are summarized in Tables 5.2 through 5.4. In each table, film gauge is varied along the horizontal row and film conductivity is varied along the vertical column. The variations in gauge and conductivity were 1.0, 5.0, 10.0, mils and .05, .10 , 1.0 W/Mk, respectively.

Table 5.2 illustrates the insulative sensitivity of particular films to the pure conduction mode, which represents a package immediately adjacent to another one. For very thin films (<1.0 mils), there is negligible change in sensitivity for Inputs #1 and #2. As the film gage increases to 5. mils and then to 10. mils, the change in sensitivity increases on the order of 10% and 20%, respectively, as the conductivity increases. Therefore, for relatively thick films, the value of conductivity is critical.

For lower conductivities (<.1 W/Mk), the sensitivity is increased by 10% as the film gauge is increased from 1 mil to 5 and

10 mils. For K_f = 1.0 W/Mk, there is no apparent change in sensitivity as the film gauge is increased.

Table 5.3 represents the results obtained for the pure convection mode. The comparison of this mode to the mode that includes radiation combined with convection will give a reliable comparison of the effect of surface radiation on package protection. This scenario is realized as a package situated on top of a stack of additional packages, subjected to free (nonforced) air currents in the freezer. There is no apparent change in sensitivity with a change of either film parameter. Consequently, in this freezer environment, a change of film thickness or conductivity is not significant. Another important factor is the calculation of the convection coefficient, h. These results have an h value of approximately 2.5 W/m^2K, which corresponds to free convection. The thermal wave propagation can be analyzed in Figure 5.9. For the response to be sensitive to any of the film parameters, the convection coefficient must be forced convection, generally on the order of 150 W/m^2K, which is unrealistic.

Table 5.4 summarizes the simulated responses associated with the combined effects of convection and radiation. This combined mode significantly effects the temperature response as shown in Figure 5.10. As was apparent for the case involving pure convection, the model is insensitive to changes in film gage and conductivity. The emmissivity factor did not become significant until Input #3 (Pulse). Although the Pulse Input is severe, the magnitude of difference in temperature response was only 1° C.

Radiation coefficients are difficult to estimate. It should be noted that radiation is a direct function of surface color, finish and texture. Radiation coefficients are best handled experimentally, with careful attention paid to environmental factors.

Pure Conduction

DELTAX = 1 mil
Kf = .1

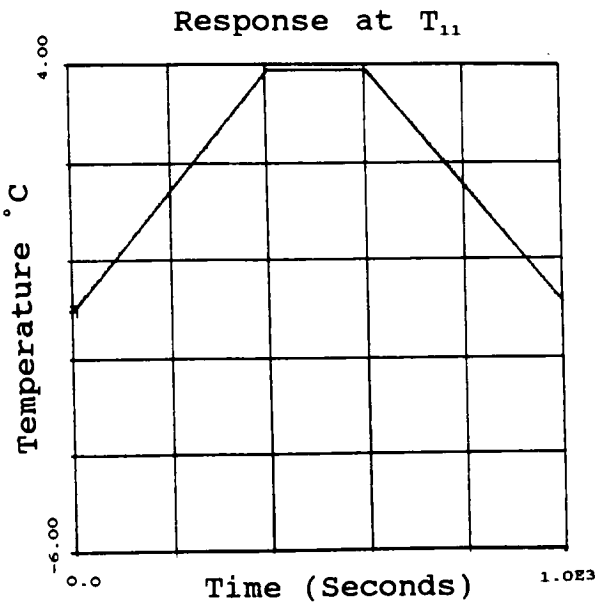

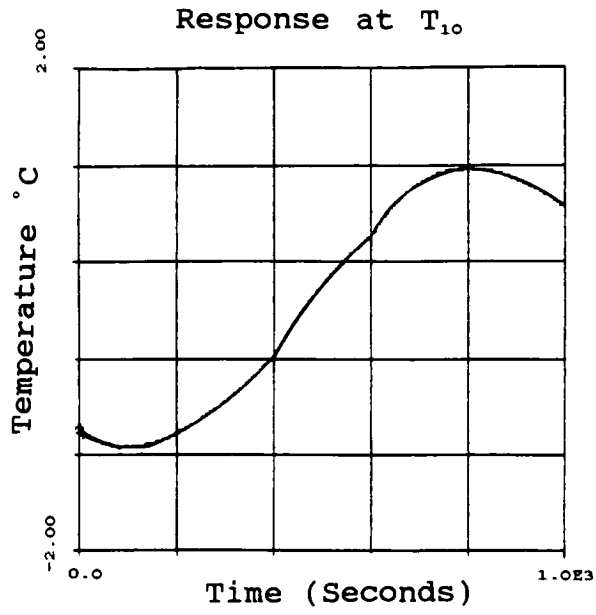

Note : Input same as Convection.

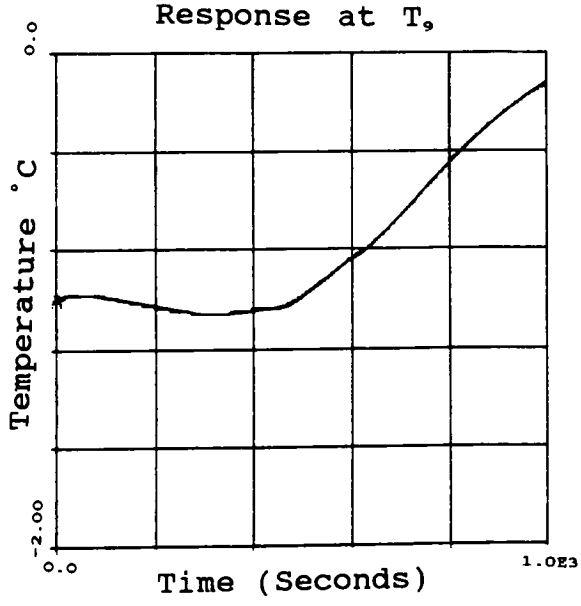

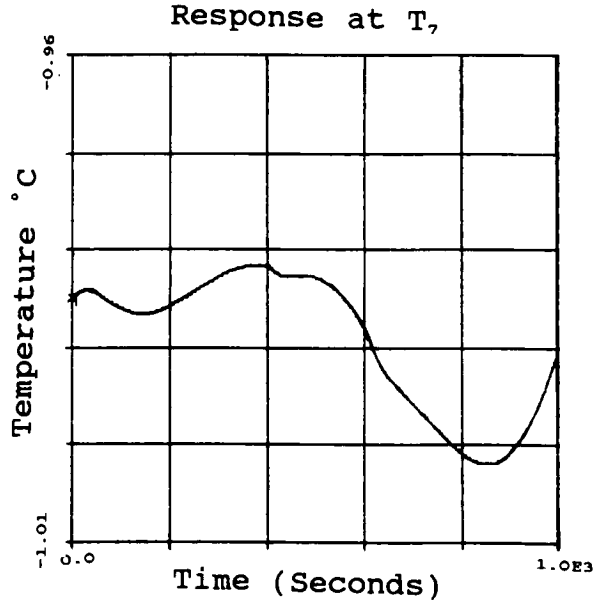

Figure 5.8
Dynamic responses of nodal temperatures.

Pure Convection

DELTAX = 1 mil
Kf = 0.1

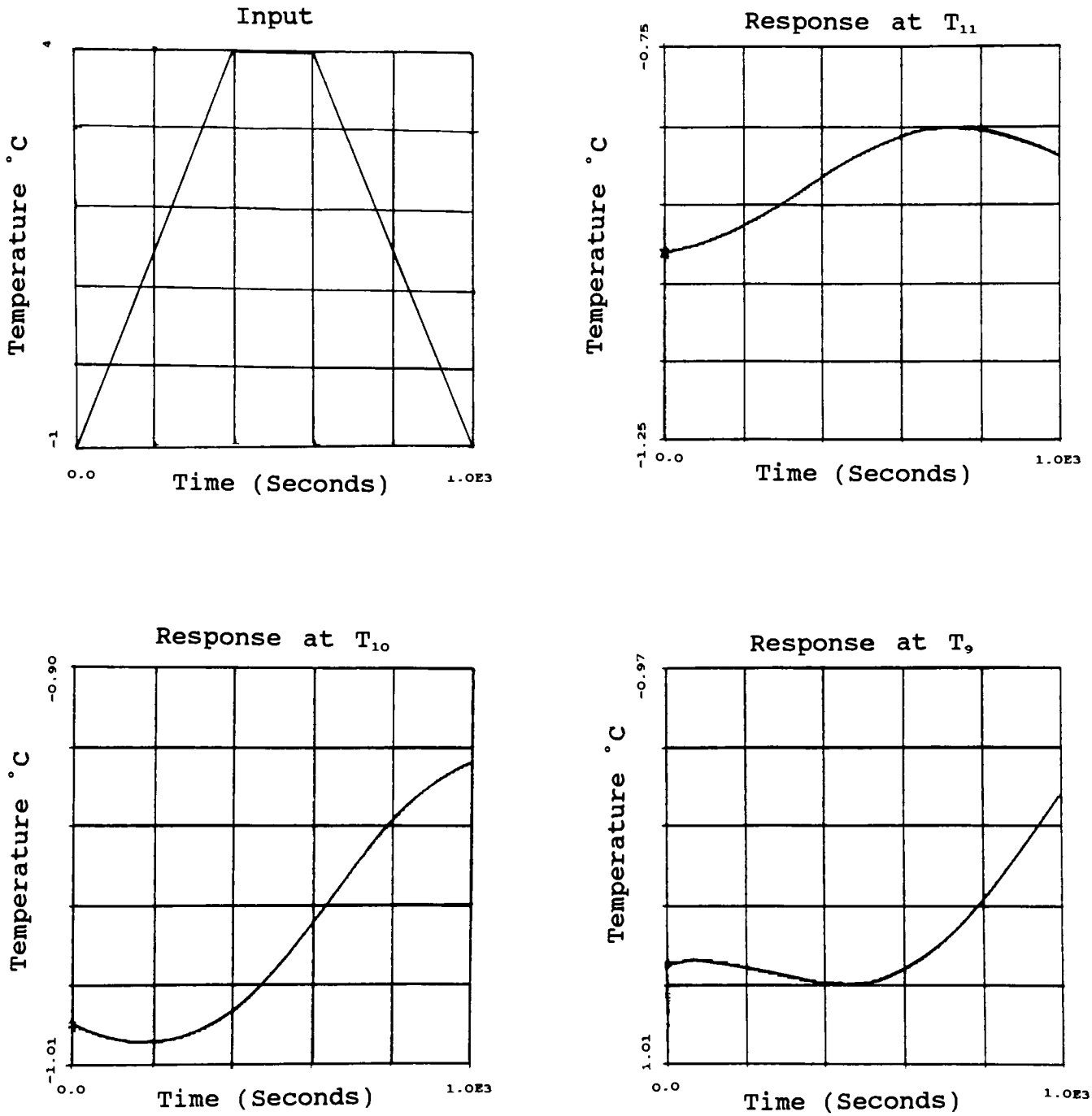

Figure 5.9
Dynamic responses of nodal temperatures.

Convection and Radiation

DELTAX = 1 mil
ϵ = 0.2
Kf = 0.1

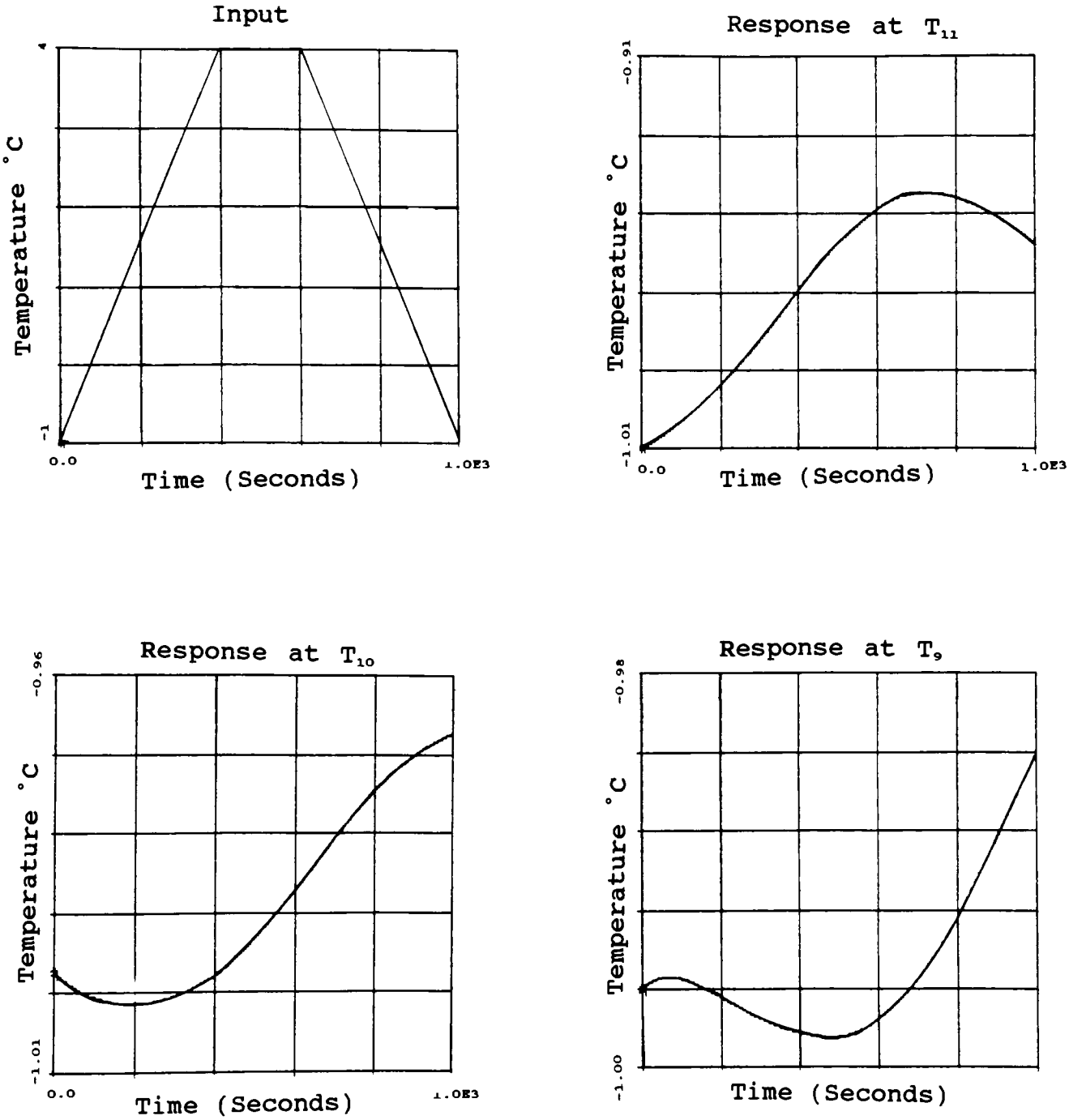

Figure 5.10
Dynamic responses of nodal temperatures.

CONDUCTION

INPUT #1 (HARMONIC)

DELTAX	1 mil	5 mil	10 mil
K_f			
.05	T_{11}= 3.871 T_{10}= 1.13	T_{11}= 3.36 T_{10}= .889	T_{11}= 2.79 T_{10}= .638
.1	T_{11}= 3.93 T_{10}= 1.165	T_{11}= 3.675 T_{10}= 1.037	T_{11}= 3.36 T_{10}= .895
1.	T_{11}= 3.993 T_{10}= 1.19	T_{11}= 3.967 T_{10}= 1.182	T_{11}= 3.933 T_{10}= 1.165

INPUT #2 (RISE-CONSTANT)

DELTAX	1 mil	5 mil	10 mil
K_f			
.05	T_{11}= 3.911 T_{10}= 1.57	T_{11}= 3.569 T_{10}= 1.303	T_{11}= 3.163 T_{10}= 1.019
1.	T_{11}= 3.996 T_{10}= 1.642	T_{11}= 3.978 T_{10}= 1.623	T_{11}= 3.953 T_{10}= 1.603

INPUT #3 (PULSE)

DELTAX	1 mil	5 mil	10 mil
K_f			
.01	T_{11}= 17.8 T_{10}= 9.36	T_{11}= 11.27 T_{10}= 4.517	T_{11}= 7.249 T_{10}= 2.506
.05	T_{11}= 19.95 T_{10}= 12.16	T_{11}= 17.82 T_{10}= 9.316	T_{11}= 15.80 T_{10}= 7.428
1.	T_{11}= 19.97 T_{10}= 13.72	T_{11}= 19.89 T_{10}= 13.26	T_{11}= 19.78 T_{10}= 12.86

Table 5.2
Summary of freezer simulation nodal temperatures.

CONVECTION

INPUT #1 (RISE-CONSTANT-FALL)

DELTAX	1 mil	5 mil	10 mil
K_f			
.1	T_{11}=-.8516 T_{10}=-.9338	T_{11}=-.8517 T_{10}=-.9339	T_{11}=-.852 T_{10}=-.9342
1.	T_{11}=-.8513 T_{10}=-.9337	T_{11}=-.8513 T_{10}=-.9337	T_{11}=-.8514 T_{10}=-.9338

INPUT #2 (RISE-CONSTANT)

DELTAX	1 mil	10 mil
K_f		
.05	T_{11}=-.7856 T_{10}=-.9175	T_{11}=-.7877 T_{10}=-.9184
1.0	T_{11}=-.7854 T_{10}=-.9174	T_{11}=-.8552 T_{10}=-.9174

INPUT #3 (PULSE)

DELTAX	1 mil	10 mil
K_f		
.01	T_{11}=-.2643 T_{10}=-.704	T_{11}=-.3030 T_{10}=-.7198
.05	T_{11}=-.2607 T_{10}=-.7027	T_{11}=-.2689 T_{10}=-.7060
1.0	T_{11}=-.2600 T_{10}=-.7024	T_{11}=-.2602 T_{10}=-.7025

Table 5.3
Summary of freezer simulation nodal temperatures.

CONVECTION & RADIATION

INPUT #1 (RISE-CONSTANT-FALL)

Emissitivity	ϵ=.2		ϵ=.9	
DELTAX	1 mil	10 mil	1 mil	10 mil
K_f				
.05	T_{11}=-.7968 T_{10}=-.909	T_{11}=-.799 T_{10}=-.910	T_{11}=-.6135 T_{10}=-.8267	T_{11}=-.6176 T_{10}=-.8267
.1	T_{11}=-.796 T_{10}=-.909	T_{11}=-.798 T_{10}=-.909	T_{11}=-.613 T_{10}=-.8267	T_{11}=-.615 T_{10}=-.8267
1.	T_{11}=-.796 T_{10}=-.9092	T_{11}=-.796 T_{10}=-.9092	T_{11}=-.613 T_{10}=-.8266	T_{11}=-.6133 T_{10}=-.8267

INPUT #2 (RISE & CONSTANT)

Emissitivity	ϵ=.2		ϵ=.9	
DELTAX	1 mil	10 mil	1 mil	10 mil
K_f				
.05	T_{11}=-.7228 T_{10}=-.8995	T_{11}=-.7250 T_{10}=-.9006	T_{11}=-.8095 T_{10}=-.4792	T_{11}=-.8115 T_{10}=-.4846
1.	T_{11}=-.7225 T_{10}=-.8993	T_{11}=-.7227 T_{10}=-.8994	T_{11}=-.8093 T_{10}=-.4787	T_{11}=-.8094 T_{10}=-.4789

INPUT #2 (PULSE)

Emissitivity	ϵ=.2		ϵ=.9	
DELTAX	1 mil	10 mil	1 mil	10 mil
K_f				
.05	T_{11}= .0359 T_{10}=-.5817	T_{11}= .0246 T_{10}=-.5863	T_{11}= 1.020 T_{10}=-.1813	T_{11}= .9989 T_{10}=-.1900
.1	T_{11}= .0365 T_{10}=-.5814	T_{11}= .0309 T_{10}=-.5837	T_{11}= 1.021 T_{10}=-.1809	T_{11}= 1.011 T_{10}=-.1852
1.	T_{11}= .0371 T_{10}=-.5812	T_{11}= .0365 T_{10}=-.5814	T_{11}= 1.022 T_{10}=-.1801	T_{11}= 1.021 T_{10}=-.1809

Table 5.4
Summary of freezer simulation nodal temperatures.

6.0 CONCLUSIONS

In reviewing the results from the experiments and mathematical modeling, the following conclusions can be stated.

1) A cavitated core film provides better insulation protection than non-core films in a conductive environment. This insulative benefit increases as gauge increases.

2) The insulated box experiment and the one-dimensional lumped parameter model showed that radiation heat transfer is significant. This significance decreases as the convection coefficient, h (W/mK), increases.

3) Results show that, metallized films can be utilized more effectively than nonmetallized films as packaging materials under conditions of sudden heat or convective/radiative environments.

4) The thermal analyzer experiment established qualitative results pertaining to the differences in conductive properties of various films. These results confirmed initial theories that a cavitated-core film was more insulative.

5) Statistically, the experimental methods proved to be very reliable. The thermal analyzer experiment could be employed for other non-packaging films used in a variety of other thin film applications such as paper copiers.

6) The semi-discrete Galerkin approximation allowed the apparent conductivities of each composite film to be estimated. Using the apparent conductivities, one is then able to find response characteristics of an individual package wrapped in an insulative film subject to various freezer environments.

7) Mathematical modeling demonstrated how important the differences in apparent conductivities are in actual freezer applications. The results from the finite element model showed that difference in conductivity, when the package is subjected to a convective and radiative environment, did not contribute to any substantial insulative differences.

8) The modeling also showed that conduction alone proved to have insulative benefits with decreasing film conductivity. As the film thickness increases, these insulative benefits become more prominent.

9) The benefits of this study go far beyond the specific packaging film results. The 10 element model allows the input of any boundary conditions (input environments) or package scenarios that might be of interest. The thermal analyzer, Galerkin approximation and finite element model can establish quick and inexpensive results for film conductivities and significance in a practical environment.

7.0 REFERENCES

[1] F.P. Incropera, D.P. DeWitt, Fundamentals of Heat and Mass Transfer, Second Edition, J. Wiley & Sons Inc., New York, pp. 3-10,35,245, Appendix A, (1985).

[2] U. Grigul, H. Sandner, Heat Conduction, Springer-Verlag, New York, pp. 1-5, (1984).

[3] C.A. Amsden, "Measurement of The Thermal Conductivity of Thin Solid Films With a Thermal Comparator," Masters Dissertation, Rochester Institute of Technology, (1988).

[4] H. Lee, "Rapid Measurement of Thermal Conductivity of Polymer Films," Rev. Sci. Instrum., Volume 53, No. 6, June 1982.

[5] J.N. Reddy, An Introduction to the Finite Element Method, McGraw-Hill, New York, Chapter 2.

8.0 APPENDIX

8.1 Fortran List Files

ACSL Program : Lumped Conv/Rad Model
Lumped parameter model representative of Insulated Box (5.1).

ACSL Program : Kcomp
Galerkin Approximation of Thermal Analyzer domains (5.3).

ACSL Program : Freeze10c
Finite Element Model of freezer commodity wrapped in insulative film with conductive boundary condition (5.4).

ACSL Program : Freeze10
Finite Element Model of freezer commodity wrapped in insulative film with convective boundary condition (5.4).

ACSL Program : Freeze10r
Finite Element Model of freezer commodity wrapped in insulative film with convective and radiative boundary condition (5.4).

```
      " DETERMINATION OF THE THERMAL PROPERTIES OF POLYMER THIN FILMS "

      " DUANE A. SWANSON, MECHANICAL ENGINEERING, ROCHESTER INSTITUTE "
                                                  " OF  TECHNOLOGY 1990"

      " THESIS FOR MASTERS OF SCIENCE "

      " Program : ACSL : RIT VAX/VMS                                    "
      " Lumped parameter model : Insulated Box                          "

      " Abstract : This ACSL file solves a model representative         "
      "   of the Insulated Box. The properties of the air and film      "
      "   are averaged together.                                        "

PROGRAM LUMPED CONV/RAD MODEL
DERIVATIVE

      CINTERVAL       CINT = 1.
      "-----------------------DEFINE PRESET VARIABLES"
      CONSTANT        TSTP = 3600., ...
                      TEMPIC = 298., ...
                      TINF = 245., ...
                      A = .0232, ...
                      V = .003375, ...
                      RHO = 1110., ...
                      C = 2370., ...
                      h = 10., ...
                      eps = 0., ...
                      sig = 5.67E-8

      "-----------------------"

      TEMPD = -(A/(rho*C*V))*( h*(TEMP - TINF) + ...

                eps*sig*(TEMP**4 - TINF**4))

      "-----------------------INTEGRATE "
      TIME = INTEG(1.,0.)
      TEMP = INTEG(TEMPD,TEMPIC)
      DLESS = (TEMP-TINF)/(TEMPIC-TINF)
      "-----------------------SPECIFY TERMINATION CONDITION"
      TERMT(T.GE.TSTP)
END $" OF DERIVATIVE "
END $" OF PROGRAM "
```

```
      " DETERMINATION OF THE THERMAL PROPERTIES OF POLYMER THIN FILMS "

      " Program : ACSL : RIT VAX/VMS  ( KCOMP.CSL )                    "
      " Thermal analyzer : Comparison of Apparent Conductivities   "

      " Abstract : This ACSL file solves three differential equations "
      "   that represent the Galerkin approximation to the two domains"
      "   representative of the two domains of the thermal analyzer.  "

      " Variables : TSTP = Total Time      HF = Film thickness         "
      "             AO,BO,CO = Initial parameters                      "
      "             L1,L2 = Domain thickness                           "
      "             D1,D2 = Depth of thermocouples                     "
      "             KA,KF = Thermal conductivity of aluminum, film     "
      "             alpha = Thermal diffusivity of aluminum            "

      "             kmin =  starting value of thermal conductivity     "
      "             kmax =  final value of thermal conductivity        "
      "             delk =  increment of thermal conductivity          "

PROGRAM KCOMP.CSL
INITIAL
      "----------- Enter values for the following 3 parameters -------"
      KMIN = .01
      KMAX = .05
      DELK = .01
      "-------------------------------------------------------------"
      KF = KMIN
      N1..Continue
END $"OF INITIAL"
DERIVATIVE

      "----------------------DEFINE PRESET VARIABLES"

      CONSTANT        TSTP = 60., AO = 0.0, ...
                      BO = 0., CO = 0.0, ...
                      L1 = .0015, ...
                      L2 = .009525, ...
                      HF = .0000254, ...
                      PI = 3.141592654, ...
                      D1 = .00127, ...
                      ALPHA = 68.2E-06, ...
                      KA = 168., ...
                      KF = .05


      CINTERVAL       CINT = .1   $ "Integrated Step"

      "--------------------"

      C1 = PI/(2.*L2)
      C2 = SIN(L1)
      C4 = SIN(L1-D1)
      C5 = SIN(PI*D1/(2.*L2))
      C6 = ALPHA*KF/(KA*HF)

      D1INT1 = ALPHA*(.5*L1+.25*SIN(2.*L1))
```

```
      D1INT2 = (.5*L1-.25*SIN(2*L1))

      D2C1 = ALPHA*PI**2/(8*L2)
      D2C2 = (8*L2 - PI**2*L2)/(2*PI**2)

      D3B1 = ALPHA*PI**2/((8-PI**2)*L2)
      D3B2 = 2*PI/(8-PI**2)
      D3B3 = 2*L2/PI

      ADOT = ((C6*(B-A*C2-40.))*C2 - A*D1INT1)/D1INT2
      CDOT = ( 2/PI*C6*(B-A*C2-40.) + C*D2C1 )/D2C2
      BDOT =  ( D3B2*C6*(B-A*C2-40.) + C*D3B1 )/ D3B3


      "-----------------------INTEGRATE "

      A = INTEG(ADOT,AO)
      B = INTEG(BDOT,BO)
      C = INTEG(CDOT,CO)

      "Temperature distribution in domain"
      TC1 = A * C4 + 60.
      TC2 = B - C*C5 + 20.

      "Dimensionsless parameter"
      DLESS = (TC2-TC1)/(19.98-TC1)

      "-----------------------SPECIFY TERMINATION CONDITION"

      TERMT(T.GE.TSTP)

END $" OF DERIVATIVE "
TERMINAL
  CALL LOGD(.TRUE.)
  KF = KF + DELK
  IF( KF .LE. KMAX) GO TO N1
END $"OF TERMINAL"

END $" OF PROGRAM "
```

```
  DETERMINATION OF THE THERMAL PROPERTIES OF POLYMER THIN FILMS    "
                                                                   "
  Program : Freeze10c : ACSL : RIT VAX/VMS                         "
  Programmer : Duane A. Swanson                                    "
                                                                   "
  Abstract : The ACSL program solves a system of ten differential  "
  equations that represent a Finite Element Model designed to      "
  estimate the transient heat transfer of a frozen commodity       "
  wrapped in an insulating film and subjected to various inputs.   "


PROGRAM FREEZEC

DERIVATIVE

      "-----------------------DEFINE PRESET VARIABLES"

      CONSTANT        TSTP = 1200., ...
                      T2O = -1.,...
                      T6O = -1.,  T10O= -1.,...
                      T3O = -1.,   T7O = -1.,  T11O= -1.01,...
                      T4O = -1.,   T8O = -1.,...
                      T5O = -1.,   T9O = -1.,...
                      HE = .015,...
                      DELTAX = 2.54E-05,...
                      PI = 3.14159,...
                      ALPHA = 3.09E-07,...
                      KF = 1.0,...
                      TAVE = -1.,...
                      TAMP = 5.,...
                      RHOC = 3.33E6

      CINTERVAL       CINT = 1.

      "-----------------------"

      C1 = ALPHA/(HE)
      C2 = 6./(HE*100.)
      MT = T/60


"  Various enviromental inputs the model can be subjected to. "

      "CASE 1 SINUSOIDAL INPUT"
      "TINF = TAVE  + TAMP*SIN(T*3.14159/600)"

      "CASE 2 STEP INPUT "
      "Y = PULSE(0.,1200.,400.)"
      "X = PULSE(400.,2400.,800.)"
      "Z = PULSE(600.,3600.,400.) "
      "TINF = TAVE + .75*Y*MT + X*5. - (.75)*Z*(MT-10.) "

      "CASE 3 PULSE INPUT "
      Y = PULSE(0.,1200.,600.)
      TINF = TAVE + Y*MT
```

```
      " TINF CASE 3 RISE INPUT "
      " TINF = TAVE + MT/2 "

      "TINF CASE 4 CONSTANT "
      "TINF = 20."

" The boundary condition associated with pure conduction.  "

      PBC=KF*(TINF-T11)/DELTAX/RHOC

" System of differential equations representing the finite element model "

      T2DOT=C2*(-C1*(60.769*T2-43.078*T3+11.543*T4-3.092*T5+.8287*T6...
             -.2221*T7+.0595*T8-.016*T9+.0046*T10-.0011*T11)...
             -.0004*PBC)

      T3DOT=C2*(-C1*(-43.078*T2+72.312*T3-46.171*T4+12.371*T5...
         -3.315*T6+.8883*T7-.2381*T8+.0641*T9-.0183*T10+.0046*T11)...
             +.0015*PBC)

      T4DOT=C2*(-C1*(+11.542*T2-46.171*T3+73.141*T4-46.393*T5...
        +12.43*T6-3.33*T7+.8928*T8-.2404*T9+.0687*T10-.0172*T11)...
            -.0057*PBC)

      T5DOT=C2*(-C1*(-3.093*T2+12.372*T3-46.393*T4+73.2*T5-46.41*T6...
           +12.436*T7-3.333*T8+.8974*T9-.2564*T10+.0641*T11)...
            +.0214*PBC)

      T6DOT=C2*(-C1*(.8267*T2-3.315*T3+12.431*T4-46.41*T5+73.205*T6...
           -46.411*T7+12.44*T8-3.35*T9+.957*T10-.2392*T11)...
           -.0797*PBC)

      T7DOT=C2*(-C1*(-.222*T2+.8883*T3-3.331*T4+12.4356*T5-46.411*T6...
           +73.21*T7-46.427*T8+12.5*T9-3.5713*T10+.8928*T11)...
           +.2976*PBC)

      T8DOT=C2*(-C1*(.0595*T2-.2381*T3+.8928*T4-3.333*T5+12.444*T6...
           -46.427*T7+73.2692*T8-46.649*T9+13.328*T10-3.332*T11)...
           -1.111*PBC)

      T9DOT=C2*(-C1*(-.016*T2+.0641*T3-.2404*T4+.8974*T5-3.3493*T6...
           +12.5*T7-46.649*T8+74.098*T9-49.7423*T10+12.435*T11)...
            +4.145*PBC)

      T10DOT=C2*(-C1*(.0046*T2-.0183*T3+.0687*T4-.2564*T5+.9569*T6...
          -3.5713*T7+13.328*T8-49.742*T9+85.6406*T10-46.4102*T11)...
          -15.47*PBC)

      T11DOT=C2*(-C1*(-.0023*T2+.0092*T3-.0343*T4+.1282*T5-.4785*T6...
          +1.7857*T7-6.6642*T8+24.8711*T9-92.8203*T10+73.2051*T11)...
            +57.735*PBC)


      "----------------------INTEGRATE "

      T2 = INTEG(T2DOT,T2O)
      T3 = INTEG(T3DOT,T3O)
      T4 = INTEG(T4DOT,T4O)
      T5 = INTEG(T5DOT,T5O)
```

```
      T6 = INTEG(T6DOT,T6O)
      T7 = INTEG(T7DOT,T7O)
      T8 = INTEG(T8DOT,T8O)
      T9 = INTEG(T9DOT,T9O)
      T10= INTEG(T10DOT,T10O)
      T11= INTEG(T11DOT,T11O)


      "----------------------SPECIFY TERMINATION CONDITION"

      TERMT(T.GE.TSTP)

END $" OF DERIVATIVE "

END $" OF PROGRAM "
```

```
      "CASE 3 TINF PULSE INPUT "
      Y = PULSE(0.,1200.,600.)
      TINF = TAVE + Y*21

      " TINF CASE 4 RISE INPUT "
      " TINF = TAVE + MT/2 "

      "TINF CASE 5 CONSTANT "
      "TINF = 20."


" The boundary condition associated with pure convection on the film. "

      PBC = KF*HAIR*(TINF-T11)/(DELTAX*HAIR+KF)/RHOC

" System of differential equations representing the 10 elements.      "

      T2DOT = C2*(-C1*(60.769*T2-43.078*T3+11.543*T4-3.092*T5+...
         .8287*T6 -.2221*T7+.0595*T8-.016*T9+.0046*T10-.0011*T11)...
             -.0004*PBC)

      T3DOT = C2*(-C1*(-43.078*T2+72.312*T3-46.171*T4+12.371*T5...
         -3.315*T6+.8883*T7-.2381*T8+.0641*T9-.0183*T10+.0046*T11)...
             +.0015*PBC)

      T4DOT = C2*(-C1*(+11.542*T2-46.171*T3+73.141*T4-46.393*T5...
        +12.43*T6-3.33*T7+.8928*T8-.2404*T9+.0687*T10-.0172*T11)...
             -.0057*PBC)

      T5DOT =C2*(-C1*(-3.093*T2+12.372*T3-46.393*T4+73.2*T5-46.41*T6...
            +12.436*T7-3.333*T8+.8974*T9-.2564*T10+.0641*T11)...
             +.0214*PBC)

      T6DOT=C2*(-C1*(.8267*T2-3.315*T3+12.431*T4-46.41*T5+73.205*T6...
            -46.411*T7+12.44*T8-3.35*T9+.957*T10-.2392*T11)...
            -.0797*PBC)

      T7DOT=C2*(-C1*(-.222*T2+.8883*T3-3.331*T4+12.4356*T5-46.411*T6...
            +73.21*T7-46.427*T8+12.5*T9-3.5713*T10+.8928*T11)...
            +.2976*PBC)

      T8DOT = C2*(-C1*(.0595*T2-.2381*T3+.8928*T4-3.333*T5+12.444*T6...
            -46.427*T7+73.2692*T8-46.649*T9+13.328*T10-3.332*T11)...
            -1.111*PBC)

      T9DOT = C2*(-C1*(-.016*T2+.0641*T3-.2404*T4+.8974*T5-3.3493*T6...
            +12.5*T7-46.649*T8+74.098*T9-49.7423*T10+12.435*T11)...
             +4.145*PBC)

      T10DOT = C2*(-C1*(.0046*T2-.0183*T3+.0687*T4-.2564*T5+.9569*T6...
           -3.5713*T7+13.328*T8-49.742*T9+85.6406*T10-46.4102*T11)...
           -15.47*PBC)

      T11DOT=C2*(-C1*(-.0023*T2+.0092*T3-.0343*T4+.1282*T5-.4785*T6...
           +1.7857*T7-6.6642*T8+24.8711*T9-92.8203*T10+73.2051*T11)...
             +57.735*PBC)


      "----------------------INTEGRATE "
```

```
      T2 = INTEG(T2DOT,T2O)
      T3 = INTEG(T3DOT,T3O)
      T4 = INTEG(T4DOT,T4O)
      T5 = INTEG(T5DOT,T5O)
      T6 = INTEG(T6DOT,T6O)
      T7 = INTEG(T7DOT,T7O)
      T8 = INTEG(T8DOT,T8O)
      T9 = INTEG(T9DOT,T9O)
      T10= INTEG(T10DOT,T10O)
      T11= INTEG(T11DOT,T11O)


      "-----------------------SPECIFY TERMINATION CONDITION"

      TERMT(T.GE.TSTP)

END $" OF DERIVATIVE "

END $" OF PROGRAM "
```

```
"  DETERMINATION OF THE THERMAL PROPERTIES OF POLYMER THIN FILMS   "
"                                                                  "
"  Program : Freeze10r : ACSL : RIT VAX/VMS                        "
"  Programmer : Duane A. Swanson                                   "
"                                                                  "
"  Abstract : The ACSL program solves a system of ten differential "
"  equations that represent a Finite Element Model designed to     "
"  estimate the transient heat transfer of a frozen commodity      "
"  wrapped in an insulating film and subjected to various inputs.  "


PROGRAM FREEZE10R

DERIVATIVE

      "-----------------------DEFINE PRESET VARIABLES"

      CONSTANT        TSTP = 1000., ...
                      T2O = -1.,...
                      T6O = -1.,  T10O= -1.,...
                      T3O = -1.,   T7O = -1.,  T11O= -1.,...
                      T4O = -1.,   T8O = -1.,...
                      T5O = -1.,   T9O = -1.,...
                      HE = .015,...
                      DELTAX = 2.54E-05,...
                      PI = 3.14159,...
                      ALPHA = 3.09E-07,...
                      KF = .10,...
                      TAVE = -1.,...
                      TAMP = 5.,...
                      KAIR = 24.3E-03,...
                      HAIR = 2.5,...
                      SIGMA = 5.67E-08,...
                      E = .2,...
                      G = 9.8,...
                      RHOC = 3.33E6

      CINTERVAL       CINT = 1.

      "-----------------------"

      C1 = ALPHA/(HE)
      C2 = 6./(HE*100.)
      C3 = E*SIGMA
      MT = T/60.

" Various input responses upon the film's outer boundary. "

      "CASE 1 HARMONIC INPUT"

      "TINF = TAVE  + TAMP*SIN(T*3.14159/600)"

      "CASE 2 PULSE INPUT "
      Y = PULSE(0.,1200.,600.)
      TINF = (TAVE + Y*21 )
```

```
    " TINF CASE 3 RISE/STEADY INPUT "
    " TINF = TAVE + MT/2 "

    "TINF CASE 4 CONSTANT "
    "TINF = 20."


The boundary condition on the outer element surface.  "
Radiation/Convection combined. "

    PBC=KF*(HAIR*(TINF-T11)+C3*((TINF+273.)**4.-(T11+273.)**4))/...
          (DELTAX*(HAIR+4*C3*(T11+273.))+KF)/RHOC

System of differential equations. "

    T2DOT = C2*(-C1*(60.769*T2-43.078*T3+11.543*T4-3.092*T5...
     +.8287*T6-.2221*T7+.0595*T8-.016*T9+.0046*T10-.0011*T11)...
           -.0004*PBC)

    T3DOT = C2*(-C1*(-43.078*T2+72.312*T3-46.171*T4+12.371*T5...
       -3.315*T6 +.8883*T7-.2381*T8+.0641*T9-.0183*T10+.0046*T11)...
           +.0015*PBC)

    T4DOT = C2*(-C1*(+11.542*T2-46.171*T3+73.141*T4-46.393*T5+...
      12.43*T6-3.33*T7+.8928*T8-.2404*T9+.0687*T10-.0172*T11)...
           -.0057*PBC)

    T5DOT=C2*(-C1*(-3.093*T2+12.372*T3-46.393*T4+73.2*T5-46.41*T6...
          +12.436*T7-3.333*T8+.8974*T9-.2564*T10+.0641*T11)...
           +.0214*PBC)

    T6DOT=C2*(-C1*(.8267*T2-3.315*T3+12.431*T4-46.41*T5+73.205*T6...
          -46.411*T7+12.44*T8-3.35*T9+.957*T10-.2392*T11)...
          -.0797*PBC)

    T7DOT=C2*(-C1*(-.222*T2+.8883*T3-3.331*T4+12.4356*T5-46.411*T6...
          +73.21*T7-46.427*T8+12.5*T9-3.5713*T10+.8928*T11)...
          +.2976*PBC)

    T8DOT=C2*(-C1*(.0595*T2-.2381*T3+.8928*T4-3.333*T5+12.444*T6...
          -46.427*T7+73.2692*T8-46.649*T9+13.328*T10-3.332*T11)...
          -1.111*PBC)

    T9DOT=C2*(-C1*(-.016*T2+.0641*T3-.2404*T4+.8974*T5-3.3493*T6...
          +12.5*T7-46.649*T8+74.098*T9-49.7423*T10+12.435*T11)...
           +4.145*PBC)

    T10DOT=C2*(-C1*(.0046*T2-.0183*T3+.0687*T4-.2564*T5+.9569*T6...
         -3.5713*T7+13.328*T8-49.742*T9+85.6406*T10-46.4102*T11)...
         -15.47*PBC)

    T11DOT=C2*(-C1*(-.0023*T2+.0092*T3-.0343*T4+.1282*T5-.4785*T6...
         +1.7857*T7-6.6642*T8+24.8711*T9-92.8203*T10+73.2051*T11)...
           +57.735*PBC)


    "----------------------INTEGRATE "

    T2 = INTEG(T2DOT,T2O)
```

```
      T3 = INTEG(T3DOT,T3O)
      T4 = INTEG(T4DOT,T4O)
      T5 = INTEG(T5DOT,T5O)
      T6 = INTEG(T6DOT,T6O)
      T7 = INTEG(T7DOT,T7O)
      T8 = INTEG(T8DOT,T8O)
      T9 = INTEG(T9DOT,T9O)
      T10= INTEG(T10DOT,T10O)
      T11= INTEG(T11DOT,T11O)


      "-----------------------SPECIFY TERMINATION CONDITION"

      TERMT(T.GE.TSTP)

END $" OF DERIVATIVE "

END $" OF PROGRAM "
```

8.2 Additional Responses

Note : Refer to Table 5.1 for thin film identity.

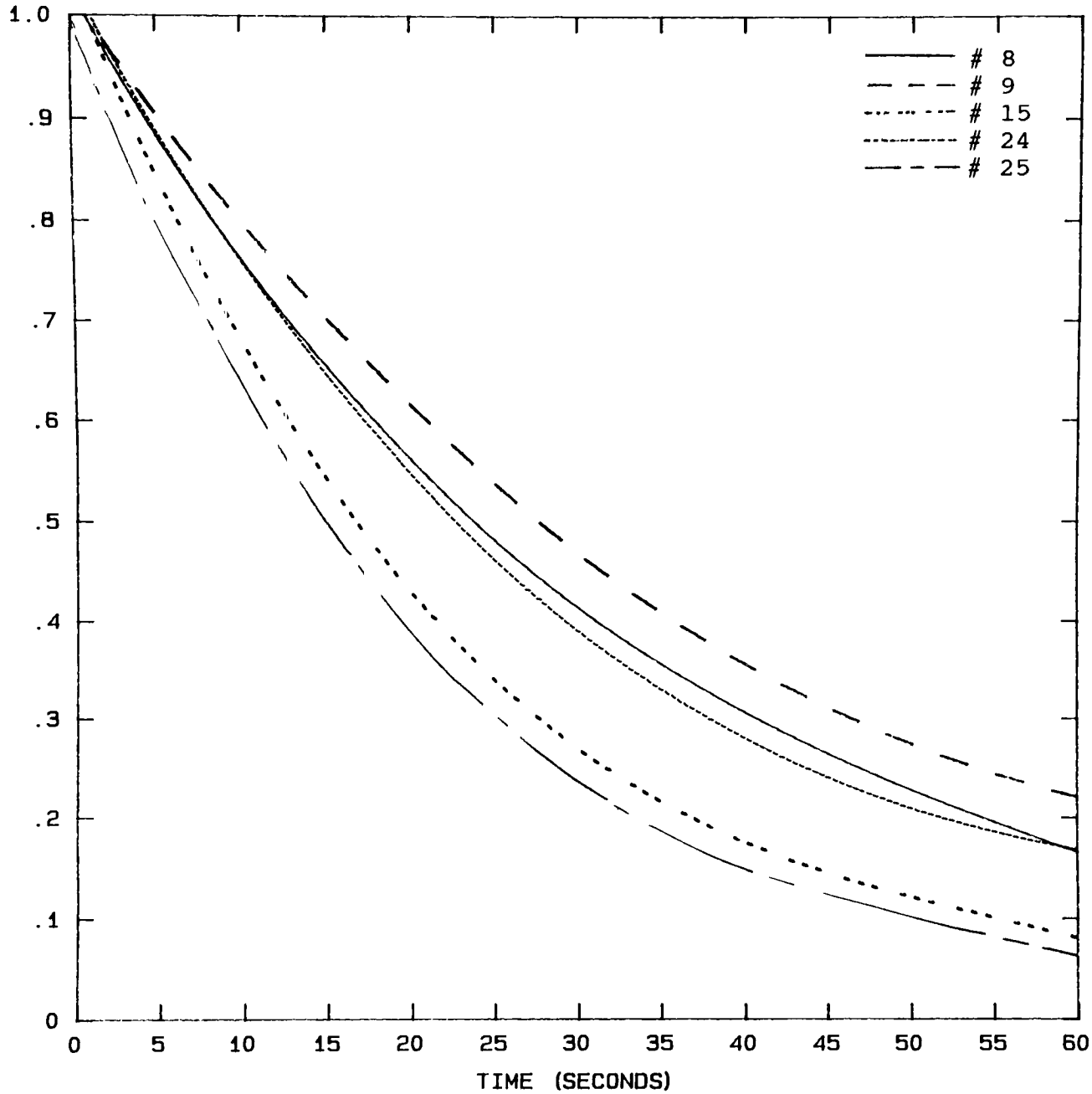
Thermal Analyzer Response of Laminated Substrates
1.0
.9
.8
.7
.6
.5
.4
.3
.2
.1
0
0
5
10
15
20
25
30
35
40
45
50
55
60
TIME (SECONDS)
$\frac{(T-T_\infty)}{(T_i-T_\infty)}$
8
9
15
24
25

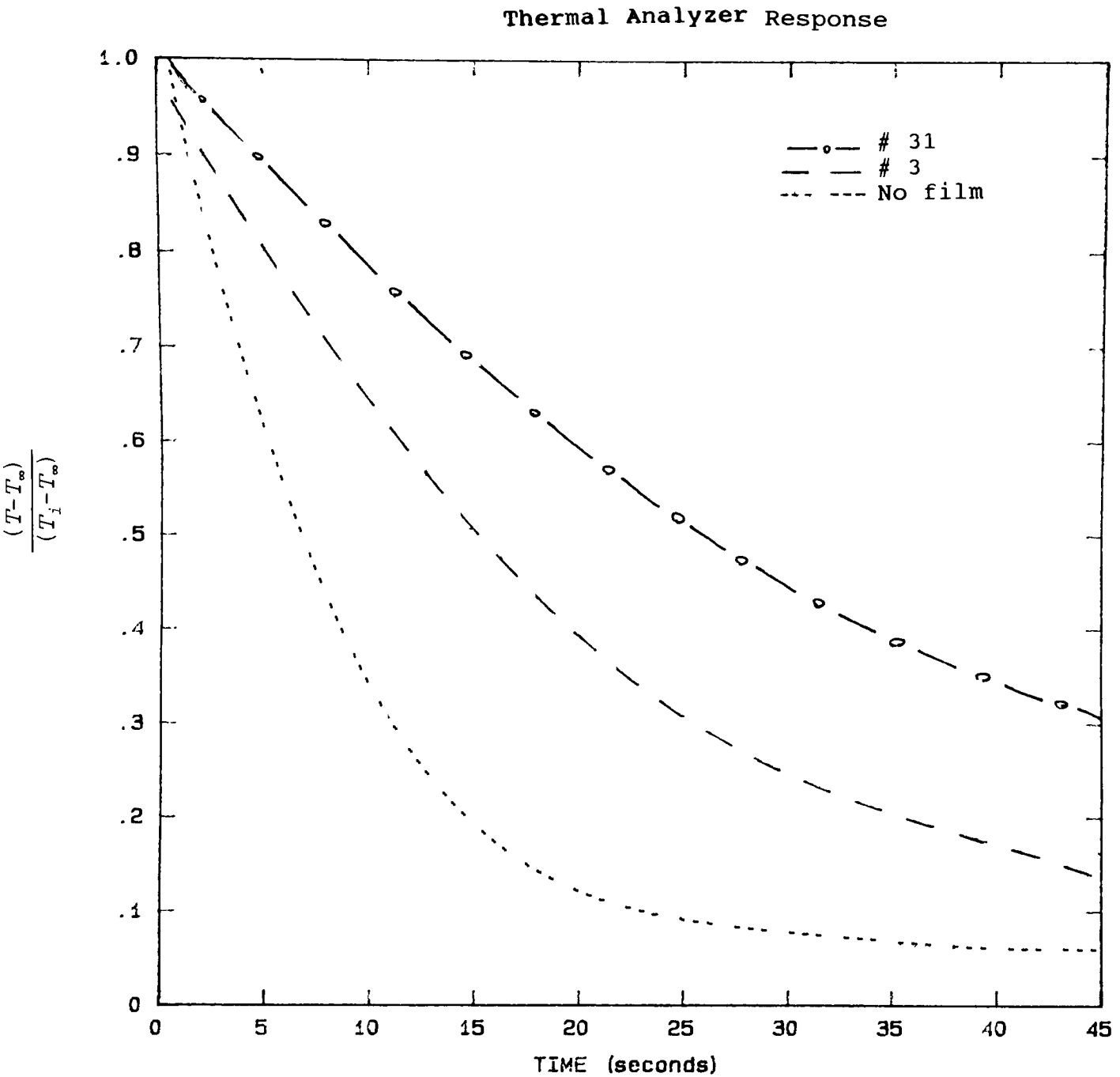
Thermal Analyzer Response
1.0
.9
.8
.7
.6
.5
.4
.3
.2
.1
0
0
5
10
15
20
25
30
35
40
45
TIME (seconds)
$\frac{(T-T_\infty)}{(T_i-T_\infty)}$
31
3
No film

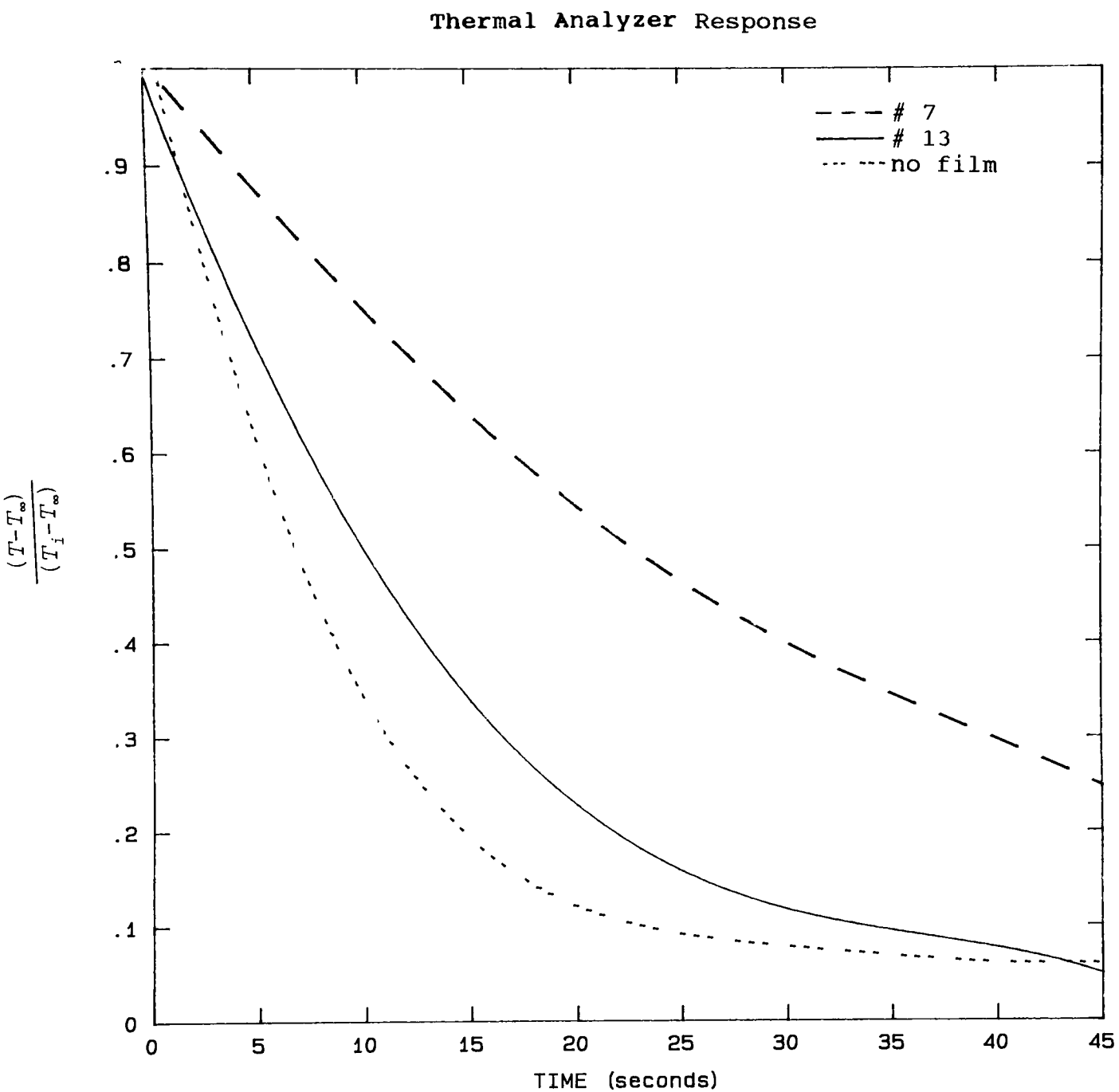
Thermal Analyzer Response
7
13
no film
$\frac{(T-T_\infty)}{(T_i-T_\infty)}$
0
.1
.2
.3
.4
.5
.6
.7
.8
.9
0
5
10
15
20
25
30
35
40
45
TIME (seconds)

Thermal Analyzer Response